effective plasma level for long periods by prevention of hepatic uptake in addition to the local administration activity.

The in vitro enzyme assay showed that the succinylated MMP inhibitor and the prodrug polymers maintained their inhibition activity for the human matrix metalloproteinases after chemical modification. Comparing the MMP inhibition activities with ONO-4817, which is only slightly soluble in water, the IC_{50} values for each of the MMPs were approximately identical. Due to the high water solubility of these water-soluble MMP inhibitors, they offer many advantages for drug dose dependent clinical trials and may suppress intimal hyperplasia when the dose concentration of the MMP inhibitors is increased. As for the prodrug polymers, since the inhibition activities showed relatively good retention they offer the potential for antirestenosis therapy. However, the IC_{50} values for the prodrug polymers indicated remarkably inferior inhibition activities against all the MMPs compared to the monomeric MMP inhibitors. Such inactivation is attributed to the steric hindrance of the MMP inhibitor moiety, which inhibits other MMP groups from binding to the enzyme's active site. **PA**, the lower **MB** contents copolymer, showed about twice as much activity as **PB**. However, copolymerization of non water-soluble synthetic MMP inhibitors, such as ONO-4817, with monomers of excellent water solubility, such as *N,N*-dimethylacrylamide, is an advantageous strategy to maintain drug concentrations at high levels in plasma and is expected to express prodrug-like controlled drug delivery functions by hydrolysis in vivo. Further in vitro studies of SMC migration assays using matrigel, in the presence of **MA**, **PA**, and **PB** are currently in progress, as are in vivo inhibition studies of experimental neointimal hyperplasia using local drug delivery systems with the infusion balloon catheter.

Experimental Section

General Methods. ^{1}H NMR spectra were recorded in DMSO-d_6 or D_2O using tetramethylsilane (0 ppm) as an internal standard with a 270 MHz NMR spectrometer (JEOL, GX-270, Tokyo, Japan) at room temperature. UV−vis absorption spectra were measured on a Pharmaspec UV-1700 spectrophotometer (Shimadzu, Kyoto, Japan). Gel permeation chromatography (GPC) analyses in *N,N*-dimethylformamide were carried out with a HPLC-8020 instrument (Tosoh, Tokyo, Japan) (column: Tosoh TSKgel α-3000 and α-5000). The columns were calibrated with narrow weight distribution poly(ethylene glycol) standards.

In Vitro Enzyme Assay. MMPs were extracted and purified from human normal dermal fibroblast. To an assayed buffer solution (40 μL) of the purified MMP (5.0 μM), *p*-aminophenylmercuric acetate (APMA: 5.0 μL, 10 mM) was added to activate the enzyme and preincubated at 37 °C for 1 h. A buffer solution (20 mL) of synthetic substrates, (7-methoxycoumarin-4-yl)acetyl-Pro-Leu-Gly-Leu-(*N*3-(2,4-dinitrophenyl)-L-2,3-diaminopropionyl)-Ala-Arg-NH_2 (McaPLDG-LDpaAR)[21] (130 μL; final concentration: 13.5 μM) with or without MMP inhibitor were incubated at 37 °C for 5 min prior to addition of the preincubated activate enzyme (50 μL/well) to each solution. The enzymatic assay was performed at 37 °C after 15 min incubation. The enzymatic activities were represented by an increase in the fluorescent intensity at 393 nm (excitation: 325 nm) per 1 min over the period of incubation. Inhibition activity, the IC_{50} values, was determined from plots of percentage inhibition vs log of inhibitor concentration.

Materials. ONO-M11-335 was kindly supplied from ONO Pharmaceutical Co., Ltd. (Osaka, Japan) and used as received. *N*-Hydroxybenztriazole (HOBt) was of special grade and purchased from Peptide Institute Inc. (Osaka, Japan) and used without further purification. 2-Aminoethyl methacrylate·HCl was purchased from Polyscience Inc., (Niles, IL) and other chemical reagents were commercially obtained from Wako Pure Chemical Industries, Ltd (Osaka, Japan). Anhydrous solvents were distilled after drying.

Synthesis: *N*-Hydroxy-5-carboxylethylcarbonyloxy-2(*S*)-methyl-4(*S*)-(4-phenoxybenzoyl)aminopentanamide (MA). To an anhydrous pyridine solution (5 mL) of ONO-M11-335 (500 mg, 1.4 mmol) was added dropwise at 0 °C an anhydrous pyridine solution (5 mL) of succinic anhydride (280 mg, 2.8 mmol), and the mixture was then stirred overnight at room temperature. The reaction mixture was diluted with AcOEt (150 mL) and washed with 1 N HCl (50 mL × 2) and then with 5% $NaHCO_3$ (50 mL × 2). The pH of the aqueous layer was adjusted to pH 5 with 1 N HCl and then extracted in AcOEt (50 mL × 2). After drying over $MgSO_4$, the solvent was removed by vacuum evaporation after filtration. The white solid was purified by silica gel column chromatography (eluent: chloroform/methanol, from 10/1 to 5/1) to give the desired product as a white solid: yield 180 mg (28%); FAB-MASS *m/n* 459.18 [M + H$^+$]; M_r = 458.47 calcd for $C_{23}H_{26}N_2O_8$; ^{1}H NMR (D_2O + Na_2CO_3) δ 0.98 (d, 3H, J = 6.9 Hz, $-CH_3$), 1.63−1.96 (m, 2H, $-CH(CH_3)CH_2-$), 2.21−2.28 (q, 1H, J = 7.2 Hz, $-CH(CH_3)-$), 2.30 (t, 2H, J = 6.0 Hz, $-CH_2CH_2CO_2H$), 2.45 (t, 2H, J = 6.0 Hz, $-CH_2CH_2CO_2H$), 4.02−4.28 (m, 3H, $-CHCH_2O-$), 6.96−7.05 (m, 4H, *m*-H of $-COC_6H_4-$ and *o*-H of $-OC_6H_5$), 7.14 (t, 1H, J = 7.5 Hz, *p*-H of $-OC_6H_5$), 7.33 (t, 2H, J = 7.5 Hz, *m*-H of $-OC_6H_5$), 7.61 (d, 2H, J = 7.5 Hz, *o*-H of $-COC_6H_4-$). Anal. ($C_{23}H_{26}N_2O_8$) C, H, N.

***N*-Hydroxy-5-[2-[*N*-[2-(isopropenylcarbonyloxy)ethyl]-carbamoyl]ethylcarbonyloxy]-2(*S*)-methyl-4(*S*)-(4-phenoxybenzoyl)aminopentanamide (MB).** To an anhydrous DMF solution (5 mL) of **MA** (778 mg, 1.7 mmol), 2-aminomethacrylate·HCl (566 mg, 3.4 mmol), HOBt (344 mg, 2.55 mmol), and NEt_3 (523 μL, 3.74 mmol) was added dropwise at −5 °C DCC (421 mg, 2.0 mmol) in anhydrous DMF (5 mL), and the mixture was stirred for 2 h followed by stirring overnight at room temperature. The reaction mixture was extracted into ethyl acetate and washed successively with three 50 mL portions of 1 N HCl, three 50 mL portions of 5% $NaHCO_3$, and 50 mL of brine, followed the separation of the organic layer, drying over $MgSO_4$, condensation, and purification by chromatography on silica gel (eluent: chloroform/methanol = 15/1) to give the desired product as a white solid: yield 536 mg (55%); FAB-MASS *m/n* 570.25 [M + H$^+$]; M_r = 569.61 calcd for $C_{29}H_{35}N_3O_9$; ^{1}H NMR (DMSO-d_6) δ 1.04 (d, 3H, J = 5.4 Hz, $-CH_3$), 1.60−1.77 (m, 2H, $-CH(CH_3)CH_2-$), 1.87 (s, 3H, $-C(CH_3)=CH_2$), 2.23−2.48 (m, 5H, $-OCOCH_2CH_2CONH-$ and $-CH(CH_3)-$), 3.31 (m, 2H, $-CONHCH_2CH_2OCO-$), 4.07−4.21 (m, 5H, $-CONHCH_2CH_2OCO-$ and $-CHCH_2O-$), 5.60 and 6.01 (s, 2H, $-C(CH_3)=CH_2$), 6.99−7.06 (t, 4H, J = 8.1 Hz, *m*-H of $-COC_6H_4-$ and *o*-H of $-OC_6H_5$), 7.17 (t, 1H, J = 8.1 Hz, *p*-H of $-OC_6H_5$), 7.43 (t, 2H, J = 8.1 Hz, *m*-H of $-OC_6H_5$), 7.82 (d, 2H, J = 8.1 Hz, *o*-H of $-COC_6H_4-$). Anal. ($C_{29}H_{35}N_3O_9$) C, H, N.

Poly[*N,N*-dimethylacrylamide-*co*-*N*-hydroxy-5-[2-[*N*-[2-(isopropenylcarbonyloxy)ethyl]carbamoyl]ethylcarbonyloxy]-2(*S*)-methyl-4(*S*)-(4-phenoxybenzoyl)aminopentanamide] (PA and PB). Two copolymers of **MB** and DMAAm were prepared by radical copolymerization. A typical procedure is as follows. A glass tube containing a mixture of **MB** (80 mg, mmol), DMAAm (250 mg, mmol), 2,2′-azobis(isobutyronitrile) (AIBN) (4.36 mg, mmol), and DMF (11 mL) was sealed under reduced pressure after three freeze−pump−thaw cycles. After shaking at 60 °C for 24 h, the precipitate, obtained by addition of ether, was separated from the solution by filtration. Reprecipitation was carried out in a DMF−ether system three times. The last precipitate was dried under vacuum. The yield of poly(AEMA-ONO-*co*-DMAAm) was 230 mg (70%). The molecular weight was estimated by GPC analysis: M_n = 18 000; ^{1}H NMR (in D_2O) δ 0.96 (d, 24H, J = 5.4 Hz, $-CH(CH_3)-$), 1.24−1.54 (m, 352H, CH_2 and CH_3 of

main chain, $-CH(CH_3)CH_2-$), 2.12–2.14 (m, 8H, $-CH(CH_3)-$), 2.31–2.98 (m, 848H, $-N(CH_3)_2$ and $-OCOCH_2CH_2CONH-$), 3.43–3.58 (m, 24H, $-CONHCH_2CH_2OCO-$ and $-CHCH_2O-$), 4.00 (m, 16H, $-CHCH_2O-$), 6.95–7.03 (2d, 32H, $J = 8.4$ Hz, *m*-H of $-COC_6H_4-$ and *o*-H of $-OC_6H_5$), 7.13 (t, 8H, $J = 8.4$ Hz, *p*-H of $-OC_6H_5$), 7.33 (t, 16H, $J = 8.4$ Hz, *m*-H of $-OC_6H_5$), 7.63 (d, 16H, $J = 8.4$ Hz, *o*-H of $-COC_6H_4-$). The degree of derivatization of MB unit was 5 mol % by UV spectral measurement. Copolymer with 10 mol % of MB unit was synthesized in a similar procedure by changing the monomer ratio in the feed (data in the text).

Acknowledgment. We thank ONO Pharmaceutical Co., Ltd. for a supply of ONO-M11-335 and measurements of MMPI activity. This study was supported in part by "Research Grants for Human Genome, Tissue Engineering Food Biotechnology", "Advanced Medical Technology", and "Aging and Health" from the Ministry of Health, Labour and Welfare of Japan and by a Grant-in-Aid for Scienific Research (B2-13450302, 2-14030095) from tne Ministry of Education, Science, Sports and Culture of Japan.

Supporting Information Available: ^1H NMR spectrum of PA. This material is available free of charge via the Internet at http://pubs.acs.org.

References

(1) Massova, I.; Kotra, L. P.; Fridman, R.; Mobashery, S. Matrix metalloproteinases: structures, evolution, and diversification. *FASEB J.* **1998**, *12*, 1075–1095. Hidalgo, M.; Eckhardt, S. G. Development of matrix metalloproteinase inhibitors in cancer therapy. *J. Natl. Cancer Inst.* **2001**, *93*, 178–193.

(2) Dollery, C. M.; McEwan, J. R.; Henney, A. M. Matrix metalloproteinases and cardiovasucular disease. *Circ. Res.* **1995**, *77*, 863–868.

(3) Galis, Z. S.; Muszynski, M.; Sukhova, G. K.; Simon-Morrissey, E.; Unemori, E. N.; Lark, M. W.; Amento, E.; Libby, P. Cytokine-stimulated human vascular smooth muscle cells synthesized a complement of enzymes required for extracellular matrix digestion. *Circ. Res.* **1994**, *75*, 181–189.

(4) Nagase, H. Activation mechanisms of matrix metalloproteinases. *Biol. Chem.* **1997**, *378*, 151–160.

(5) Sato, H.; Takino, T.; Okada, Y.; Cao, J.; Shinagawa, A.; Yamamoto, E.; Seiki M. A matrix metalloproteinase expressed on the surface of invasive tumour cells. *Nature* **1994**, *370*, 61–65.

(6) Baker, A. H.; Zaltsman, A. B.; George, S. J.; Newby, A. C. Divergent effects of tissue inhibitor of metalloproteinase-1, -2 or -3 overexpression on rat vascular smooth muscle cell invasion, proliferation, and death in vivo. *J. Clin. Invest.* **1998**, *101*, 1478–1487.

(7) Supuran, C. T.; Scozzafava, A. In *Matrix metalloproteinases (MMPs) in proteinase and peptidase inhibition: Recent potential targets for drug development*; Smith, H. J., Simons, C., Eds.; Taylor & Francis: London & New York, 2002; pp 35–61. Whittaker, M.; Floyd, C. D.; Brown, P.; Gearing, A. J. Design and therapeutic application of matrix metalloproteinase inhibitors. *Chem. Rev.* **1999**, *99*, 2735–2776.

(8) Matter, H.; Schwab, W.; Barbier, D.; Billen, G.; Hasse, B.; Neises, B.; Schudok, M.; Thorwart, W.; Schreuder, H.; Brachvogel, V.; Lonze, P.; Weithmann, KU. Quantitative structure–activity relationship of human neutrophil collagenase (MMP-8) inhibitors using comparative molecular field analysis and X-ray structure analysis. *J. Med. Chem.* **1999**, *42*, 1908–1920.

(9) Gavuzzo, E.; Pochetti, G.; Mazza, F.; Gallina, C.; Gorini, B.; D'Alessio, S.; Pieper, M.; Tschesche, H.; Tucker, P. A. Two crystal structures of human neutrophil collagenase, one complexed with a prime- and the other with an unprimed-side inhibitor: implications for drug design. *J. Med. Chem.* **2000**, *43*, 3377–3385.

(10) Jia, MC.; Schwartz, M. A.; Sang, Q. A. Suppression of human microvascular endothelial cell invasion and morphogenesis with synthetic matrixin inhibitors. Targeting angiogenesis with MMP inhibitors. *Adv. Exp. Med. Biol.* **2000**, *476*, 181–94. Graf von Roedern, E.; Grams, F.; Brandstetter, H.; Moroder, L. Design and synthesis of malonic acid-based inhibitors of human neutrophil collagenase (MMP8). *J. Med. Chem.* **1998**, *41*, 339–345.

(11) Poon, M.; Sun, J.; Marx, S. O.; Gallo, R.; Badimon, J. J.; Taubman, M. B.; Marks, A. R. Rapamycin inhibits vascular smooth muscle cell migration. *J. Clin. Invest.* **1996**, *98*, 2277–2283. Sun, J.; Marx, S. O.; Chen, H.-J.; Poon, M.; Marks, A. R.; Rabbani, L. E. Role for $p27^{Kip1}$ in vascular muscle cell migration. *Circulation* **2001**, *103*, 2967–2972.

(12) Marx, S. O.; Marks, A. R. The development of Rapamycin and its application to stent restenosis. *Circulation* **2001**, *104*, 852–855.

(13) Sierevogel, M. J.; Pasterkamp, G.; Velema, E.; de Jaegere, P. P. T.; de Smet, B. J. G. L.; Verheijen, J. H.; de Kleijn, D. P. V.; Borst, C. Oral matrix metalloproteinase inhibition and arterial remodeling after angioplasty. *Circulation* **2001**, *103*, 302–27. Margolin, L.; Fishbein, I.; Banai, S.; Golomb, G.; Reich, R.; Perez, L. S.; Gertz, S. D. Metalloproteinase inhibitor attenuates neointima formation and constrictive remodeling after angioplasty in rats: augmentative effect of $\alpha_v\beta_3$ receptor blockade. *Atherosclerosis* **2002**, *163*, 269–277.

(14) Li, C.; Cantor, W. J.; Nili, N.; Robinson, R.; Fenkell, L.; Tran, Y. L.; Whittingham, H. A.; Tsui, W.; Cheema, A. N.; Sparkes, J. D.; Pritzker, K.; Levy, D. E.; Strauss, B. H. Arterial repair after stenting and the effects of GM6001, a matrix metalloproteinase inhibitor. *J. Am. Col. Card.* **2002**, *39*, 1852–1858.

(15) Yamada, A.; Uegaki, A.; Nakamura, T.; Ogawa, K. ONO-4817, an orally active matrix metalloproteinase inhibitor, prevents lipopolysaccharide-induced proteoglycan release from the joint cartilage in guinea pigs. *Inflamm. Res.* **2000**, 49, 144–146. Mori, T.; Yamasaki, S.; Masui, F.; Matsuda, M.; Sasabe, H.; Zhou, Y. F. Suppression of the development of experimentally induced uterine adenomyosis by a novel matrix metalloproteinase inhibitor, ONO-4817, in mice. *Exp. Biol. Med.* **2001**, *226*, 429–433. Muraishi, Y.; Mitani, N.; Fuse, H.; Saiki, I. Effect of a matrix metalloproteinase inhibitor (ONO-4817) on lung metastasis of murine renal cell carcinoma. *Anticancer Res.* **2001**, *21*, 3845–52. Sawada, S.; Murakami, K.; Yamaura, T.; Mitani, N.; Tsukada, K.; Saiki, I. Therapeutic and analysis model of intrahepatic metastasis reflects clinical behavior of hepatocellular carcinoma. *Jpn. J. Cancer Res.* **2002**, *93*, 190–197.

(16) Noguchi, T.; Yasuda, S.; Itoh, T.; Arai, T.; Kanda, K.; Tsutsui, N.; Nakayama, Y.; Nonogi, H.; Matsuda, T. New multifunctional percutaneous transluminal coronary angioplasty catheter device capable of balloon infusion, local drug delivery and coronary perfusion. *J. Cardiol.* **2000**, *35*, 41–45.

(17) Yasuda, S.; Noguchi, T.; Gohda, M.; Arai, T.; Tsutsui, N.; Nakayama, Y.; Matsuda, T.; Nonogi, H. Local delivery of low-dose docetaxel, a novel microtubule polymerizing agent, reduces neointimal hyperplasia in a balloon-injured rabbit iliac artery model. *Cardiovasc. Res.* **2002**, *53*, 481–486.

(18) Yasuda, S.; Kanna, M.; Sakuragi, S.; Kojima, S.; Nakayama, Y.; Miyazaki, S.; Matsuda, T.; Kangawa, K.; Nonogi, H. Local delivery of single low-dose of C-type natriuretic peptide, an endogenous vascular modulator, inhibits neointimal hyperplasia in a balloon-injured rabbit iliac artery model. *J. Cardiovasc. Pharmacol.* **2002**, *39*, 784–788.

(19) Gottsauner-Wolf, M.; Jang, Y.; Penn, M. S.; Kaplan, A.; Ellis, S. G.; Chisolm G. M.; Topol, E. J.; Lincoff, A. M. Quantitative evaluation of local drug delivery using the infusa sleeve catheter. *Cathet. Cardiovasc. Diagn.* **1997**, *42*, 102–108. Suzuki, T.; Kopia, G.; Hayashi, S.; Baily, L. R.; Llanos, G.; Wilensky, R.; Klugherz, B. D.; Papandreou, G.; Nayaran, P.; Leon, M. B.; Yeung, A. C.; Tio, F.; Tsao, P. S.; Falotico, R.; Carter A. J. Stent-based delivery of sirolimus reduces neointimal formation in a porcine coronary model. *Circulation* **2001**, *104*, 1188–1193.

(20) Scozzafava, A.; Menabuoni, L.; Mincione, F.; Briganti, F.; Mincione, G.; Supuran, C. T. Carbonic anhydrase inhibitors. Synthesis of water-soluble, topically effective, intraocular pressure-lowering aromatic/heterocyclic sulfonamides containing cationic or anionic moieties: is the tail more important than the ring? *J. Med. Chem.* **1999**, *42*, 2641–2650. Pouticello, G. S.; Freedman, M. B.; Habecker, C. N.; Lyle, P. A.; Schwam, H.; Varga, S. L.; Christy, M. E.; Randall, W. C.; Baldwin, J. J. Thienothiopyran-2-sulfonamides: A novel class of water-soluble carbonic anhydrase inhibitors. *J. Med. Chem.* **1987**, *30*, 591–597.

(21) Knight, C. G.; Willenbrock, F.; Murphy, G. A novel coumarin-labeled peptide for sensitive continuous assay of the matrix metaloproteinases. *FEBS Lett.* **1992**, *296*, 263–266.

JM020356G

Fabrication of micropored elastomeric film-covered stents and acute-phase performances

Yasuhide Nakayama,[1*] Shogo Nishi,[2*] Hatsue Ueda-Ishibashi,[3] Takehisa Matsuda[4]
[1]*Department of Bioengineering, National Cardiovascular Center Research Institute, 5-7-1 Fujishiro-dai, Suita, Osaka 565-8565, Japan*
[2]*Department of Neurosurgery, Takatsuki Sekijyuji Hospital, 1-1-1 Abuno, Takatuki, Osaka 569-1096, Japan*
[3]*Department of Pathology, National Cardiovascular Center Hospital, 5-7-1 Fujishiro-dai, Suita, Osaka 565-8565, Japan*
[4]*Department of Biomedical Engineering, Graduate School of Medicine, Kyushu University, 3-1-1 Maidashi, Higashi-ku, Fukuoka 812-8582, Japan*

Received 4 February 2002; accepted 27 February 2002

Abstract: To prevent thrombus formation in the acute phase and restenosis in the subacute to chronic phase after stenting of atherosclerotic arteries, we developed a covered stent with a micropored elastomeric film, the blood-contacting surface of which was coated with a photocured gelatin layer immobilized with heparin. Segmented polyurethane (SPU) film (30 μm in wall thickness) as a cover material was multiply micropored by excimer laser-directed microprocessing (pore diameter, 30 μm; interpore distance, 125 μm). An aqueous mixed solution of benzophenone-derivatized gelatin and heparin was coated on the micropored SPU film. Upon ultraviolet light irradiation, a thin layer of a gelatin gel immobilized with heparin was formed and simultaneously fixed on the SPU film. The fully covered stents were assembled by wrapping a balloon-expandable stent with gelatin/heparin gel-layered SPU film and subsequently suturing and then gluing. To assess the validity of this covered stent *in vivo*, "half-covered" stents, in which half at the distal side was covered with the gel-layered SPU film, was implanted in rabbit common carotid arteries (about 3 mm in diameter). After 3 months of implantation, all the half-covered stents ($n = 7$) were patent. Regardless of the covered or noncovered region of the stents, the entire luminal surface of the stents was fully endothelialized and a thin neointimal tissue was formed. The potential advantages of a covered stent as designed above are discussed. © 2002 Wiley Periodicals, Inc. J Biomed Mater Res 64A: 52–61, 2003

Key words: stent; cover; micropore; drug delivery; elastomeric polymer

INTRODUCTION

Percutaneous transluminal angioplasty in the coronary and peripheral arteries (PTCA or PTA) using either balloon catheters or metallic stents has been widely used for the clinical treatment of atherosclerotic stenosis.[1–6] Because of the reduced incidence of restenosis derived from excessive tissue ingrowth (intimal hyperplasia), endovascular metallic stenting has become more popular than balloon angioplasty (restenosis rate within 6 months after treatment: 25–30% for stent versus 30–50% for balloon). Many technical efforts aiming at a further-reduced restenosis rate have been made, especially in the structural design[7–10] of stents and biocompatible[7,11–13] and pharmacological coating[14–29] designs for struts of stents. In general, to minimize intimal hyperplasia, at least the following two factors should be incorporated into a stent design: 1. prevention of thrombus formation on the struts in the early implantation period, and 2. pharmacological effects minimizing tissue growth including cell proliferation and extracellular matrix production. The first one is particularly important because platelet-derived growth factor secreted from aggregated platelets in the thrombus is a potent mitogenic substance for smooth muscle cells (SMCs) which is one of the principal cells triggering intimal hyperplasia.[30,31] Previous articles have reported promising approaches via biocompatible designs including heparin derivatization and immobilization on struts,[23–27] thus minimizing thrombus formation, and pharmacological coatings[14–29] including sustained release of anti-cancer agents such as metalloproteinase inhibitor[15,16] and taxol,[21,22] thus

Correspondence to: T. Matsuda; e-mail: matsuda@med.kyushu-u.ac.jp
Contract grant sponsor: Promotion of Fundamental Studies in Health Science of the Organization for Pharmaceutical Safety and Research; contract grant number: 97-15
*Authors have contributed equally to this study.

reducing cell proliferation. The unexplored factor is 3. to construct or place a physical barrier[7–9] for the prevention or reduction of tissue ingrowth at the blood/stent interface.

Our attempts to reduce the restenosis rate of stents can be divided into two strategetic approaches: one approach is a photocured coating for struts,[19] which permits drug release and gene transfer. To this end, styrenated gelatin,[32,33] which was originally designed as a photocurable glue and a tissue-engineered scaffold, was mixed with model substances, such as protein and gene-encoding adenovirus, and photocured on struts by visible light-induced radical polymerization. Upon implantation in arteries, time-dependent permeation of a model protein and gene transfection from the stent-facing tissue to a deeper vascular tissue as well as a prolo ıged period of gene expression were noticed. Thus, photocurable gelatin served as a drug- or gene-delivery matrix.

The other approach under development is the loading of a physical barrier against tissue ingrowth on a stent, as mentioned above, which is also expected to serve as a pharmacological reservoir for drug or gene delivery. To this end, segmented polyurethane (SPU) elastomeric thin film with well-designed and fabricated micropores is wrapped to form a "covered" stent. This is based on our previous studies in which such a micropored SPU tube was photocured. Benzophenone-derivatized gelatin[34] mixed with heparin served as a small-diameter compliant graft[35,36] (wall thickness, 100 μm; inner diameter, 1.5 mm), and very high patency and rapid normal tissue regeneration without substantial intimal hyperplasia in arterial circulatory system were achieved. In this study, this heparin-loaded photocured gelatin-coated thin SPU film was used to cover a stent.

In contract, nonpermeable (or nonmicropored) artificial grafts provided very low patency. Our previous *in vivo* study[8] using a covered stent with regionally different pore densities showed that a higher pore density results in a lower degree of intimal hyperplasia under the particular condition of micrporosity densities examined. Based on these previous data, we developed a covered stent with a micropored elastomeric thin film and drug delivery function.

In this report, first we describe the fabrication method of the covered stent. Second, as a model device, we prepared "half-covered" stents in which half of each stent at the distal side was covered with the micropored film, and implanted them in the common carotid arteries of rabbits. This enabled us to demonstrate the validity of the concept of the covered stent with high reliability. That is, the effect of the covering on neointimal hyperplasia can be examined in a single animal using a single device by implantation of such a half-covered stent, thus minimizing the number of animal experiments and verifying our concept with high fidelity.

EXPERIMENTAL

Preparation of covered stents

SPU film (thickness, 30 μm; size, 15 × 7 mm; Sheedom Co., Tokyo, Japan) was used as the covering material, and microporing (diameter, 30 μm; interpore distance, 125 μm) of the film was performed using a KrF excimer laser microprocessing apparatus (model L4500; Hamamatsu Photonics, Hamamatsu, Japan).[37] One side of the micropored SPU film was coated with an aqueous solution (20 $\mu L/cm^2$) of benzophenone-derivatized gelatin[34] (benzophenone groups per gelatin molecule, 32 groups; 50 mg/mL) and heparin (25 mg/mL, 164.5 μ/mg; Wako Pure Chemical Ind., Osaka, Japan) and irradiated with a 400-W ultra-high-pressure mercury-vapor lamp (H-400-A/B; Irie Co., Tokyo, Japan). The treated surface of the film was placed on the outside of a balloon-expandable stent (Palmaz-Schatz; length, 15 mm; diameter, 1.2 mm; Johnson & Johnson Interventional Systems, Warren, NJ), and stay-sutured using 10-0 nylon thread under microscopy at six points. The film ends were overlapped, and adhered using a small amount of *N,N*-dimethylformamide (DMF) which is a good solvent for SPU, to prepare the covered stents.

Implantation

The experimental animals were seven New Zealand white rabbits, weighing 3–4 kg. The investigations were performed according to the Principles of Laboratory Animal Care (formulated by the National Society for Medical Research) and the Guide for the Care and Use of Laboratory Animals (National Institutes of Health Publication, No. 56-23, revised 1985). Heparin (2000 IU) was administered only during angiography. The covered stent mounted on a PTA balloon catheter (3.0 mm, 2 cm, SAVVY, Johnson & Johnson) was advanced into the common carotid artery (approximately 3 mm) from the femoral artery under fluoroscopy using a standard PTCA microguidewire. The balloon was inflated at a pressure of 8 atm for 30 s, deflated, and slowly withdrawn, leaving the covered stent in place. Neither antiplatelet agents nor additional anticoagulants were administerd during the 3-month follow-up period.

Microscopic examination

The implanted stents, including the surrounding common carotid artery tissues, were dissected free

and fixed with 10% formaldehyde in phosphate buffer (pH 7.4) for more than 48 h for light microscopy and scanning electron microscopy (SEM). Specimens for light microscopy were dehydrated with an alcohol series and embedded in glycolmethacrylate. Thin sections of the tissues were prepared in the direction of the circumference, subjected to standard hematoxylin and eosin staining, and observed under a light microscope (VANOX-S; OLYMPUS, Tokyo, Japan). Specimens for SEM were postfixed with 1% osmium tetraoxide, dehydrated in a graded series of ethanol, critical point dried, and sputter coated with platinum.

Morphometry

Using the National Institutes of Health Image software after calibration the thickness of the neointimal layer, defined as the distance between the endothelial lining and the stent strut or internal elastic lamina, was measured on top of and between the stent struts in at least three hematoxylin and eosin-stained sections at the proximal portion (bared region in the stent) and the distal portion (covered region) of each stented carotid segment.

Mechanical properties

The measurements of the tensile strength and the apparent elastic modulus of the SPU films were performed using a rheometer (RE-3305; Yamaden, Tokyo, Japan). The stress was recorded by continuous loading of strain to the films at a rate of 0.5 mm/s up to about 4 times extension. Apparent elastic modulus of the films were determined using the slope of the linear part of the strain–stress curve obtained at the initial extension.

RESULTS

Fabrication procedure

The fabrication procedure of the covered stent is shown in Figure 1, and the outline is described below. SPU film used as a covering film was subjected to laser ablation to create multiple micropores of a defined size (30 μm in diameter) and pore distribution (interpore distance, 125 μm) (step I in Fig. 1). Coating of a mixed aqueous solution of benzophenone-derivatized gelatin[34] and heparin and subsequent ultraviolet (UV) irradiation on one face of the micropored film produced a crosslinked gelatin layer which was immobilized with heparin (step II). A commercially available balloon-expandable stent was wrapped with the microporous SPU film with its treated surface facing inwards (step III). One end of the film was fixed to the stent strut by suturing (step IV). The other end was overlapped with the fixed end and adhered to it by gluing with DMF (step V). The detailed procedures for each step are described below.

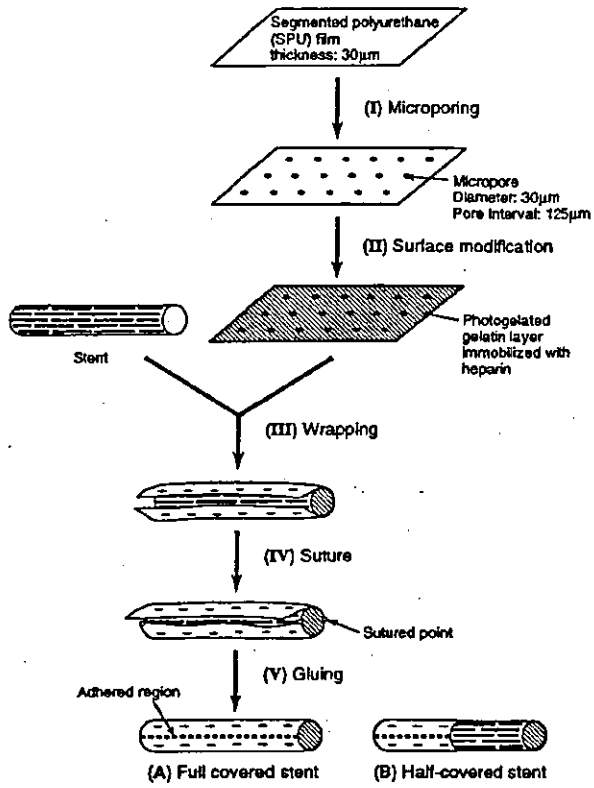

Figure 1. A schematic diagram of the preparation of the covered stent by microporing of SPU film with ablation by excimer laser (I), surface heparin immobilization using benzophenone-derivatized gelatin by UV irradiation (II), followed by covering the treated SPU film on a balloon-expandable stent (III, IV, V).

Microporing of the cover film (step I)

Microporing of the cover film was performed using a previously developed excimer laser ablation technique.[37] Irradiation of pulsed UV light from the excimer laser processing apparatus through a photomask with a round aperture 660 μm in diameter produced a micropattern of micropores 30 μm in diameter and with an interpore distance of 125 μm [Fig. 2(a, b)]. The mechanical properties of the micropored SPU films produced were examined by tensile strength tests. As shown in Figure 3, upon stretching the film, the strain of the film increased and concomi-

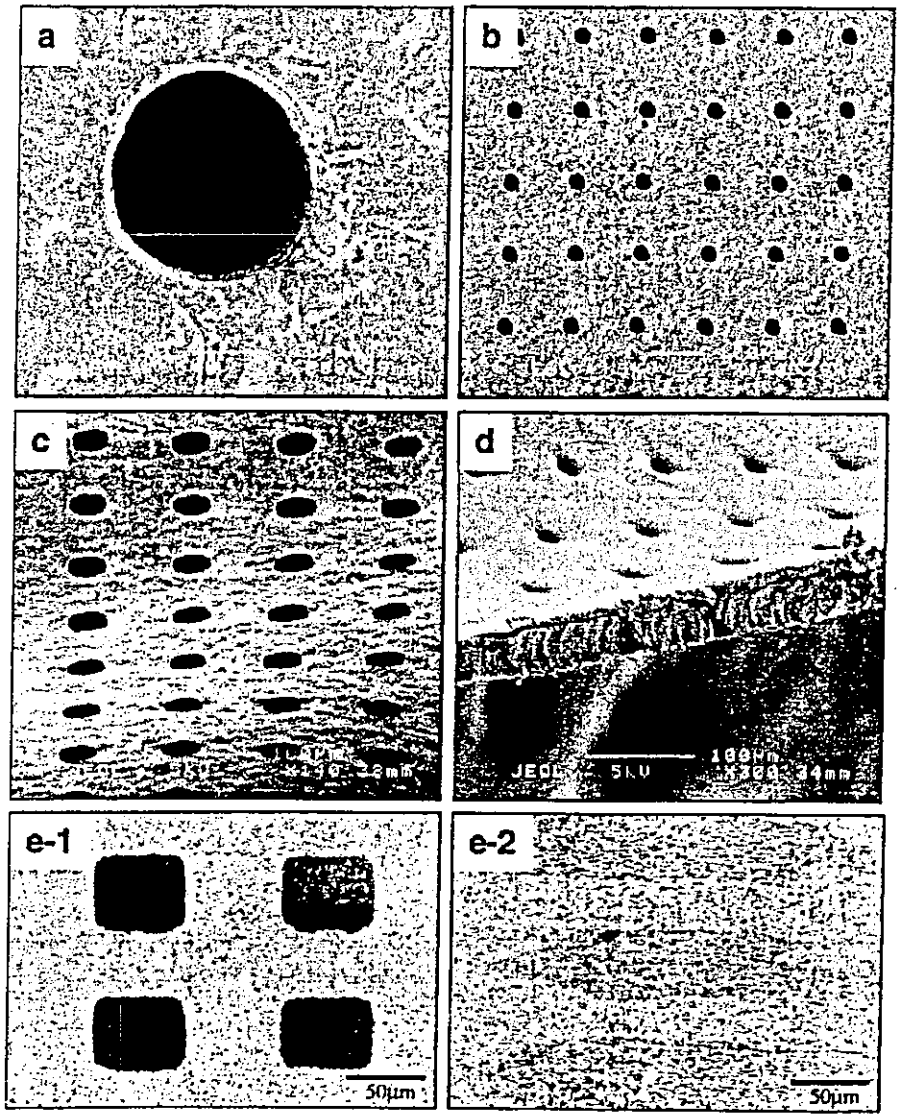

Figure 2. SEM of (a) the micropore and (b) multiple micropores, all of which were prepared by ablation with an excimer laser of SPU films, (c) multiply micropored SPU film after expanded upon about 4-times stretching from the original dimension in b, and (d) cross-section of the micropored SPU film surface-fixed with a heparin-immobilized gelatin layer, which was prepared by coating with the mixture of benzophenone-derivatized gelatin and heparin on the micropored SPU film and subsequent UV irradiation. Light micrographs of the SPU film partially surface-fixed with heparin-immobilized gelatin gel layer before (e-1) and after (e-2) stretching. The gelatin gel layer was fixed on only the dark-colored rectangular areas in e-1.

tantly the micropores were deformed from circles to ellipses [Fig. 2(c)]. The stress increased almost linearly within a range of strain up to 0.5, and the film was not ruptured by up to about 4 times of stretching from the original dimension. The elastic coefficient calculated was 1.60×10^7 Pa for the non-micropored film and 1.45×10^7 Pa for the micropored film.

Heparin immobilization on the cover film (step II)

One side of the microporous SPU film was coated with the aqueous solution of benzophenone-derivatized gelatin[34] and heparin, dried, and subsequently irradiated with UV light. The irradiated surface was slightly swollen in water, indicating the formation of a water-swellable gelatin gel layer. No delamination even upon vigorous rinsing with water was observed, indicating that the gelatin layer was tightly fixed to the SPU surface. SEM of the cross-section of the treated SPU film revealed that an approximately 5-μm-thick gelatin gel layer was formed on the coated surface, and the micropores were completely filled by the photocured gel [Fig. 2(d)]. To visualize heparin immobilized in the gel layer, the fol-

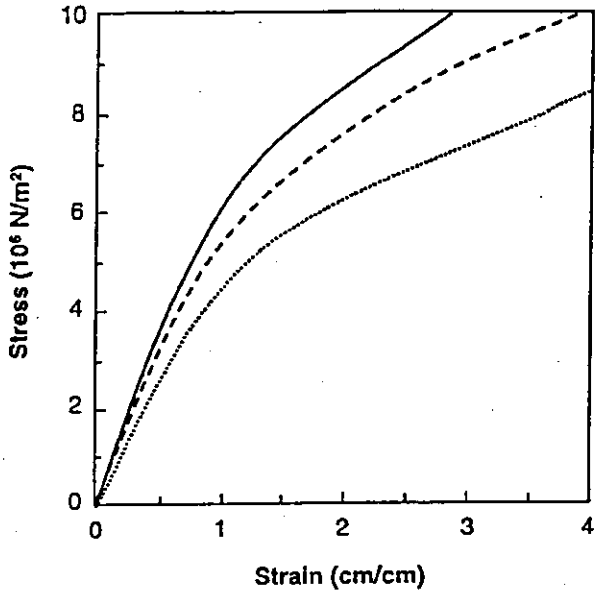

Figure 3. Stress–strain curves of nontreated SPU film (—), the micropored SPU films with an interpore distance of 125 μm (- - -), and the adhered SPU film (—). All films were expanded at a constant rate (0.5 mm/min) up to about 4-times stretching.

lowing experiment was separately conducted. The gelatin gel layer containing heparin was regionally prepared on SPU film by UV irradiation through a photomask with a lattice pattern, washed to remove non-photocured gelatin mixture, and immersed in an aqueous solution of a cationic dye, toluidine blue.[38] A blue–purple-stained lattice pattern was formed only at the gelatin-fixed area [Fig. 2(e-1)]. However, the film fixed with the gelatin without heparin was not stained by toluidine blue (data not shown). These results indicate that the formation of heparin-immobilized gel and fixation on SPU film simultaneously occurred by UV irradiation. When such a gelatin-fixed film was stretched, the gelatin layer was also synchronously stretched without delamination [Fig. 2 (e-2)].

Assembling of the covered stents (steps III, IV, V)

The heparin-immobilized gelatin gel layer-coated SPU film was placed so as to face the struts of stent, and one end of the film was wrapped and sutured to the struts at three sites using 10-0 nylon thread under microscopy. After the stent was tightly wrapped with the SPU film, the free ends of the film with a width of about 1 mm were overlapped, and adhered by gluing with DMF. The adhesion strength of the adhered SPU film was examined by tensile strength tests as described above. There was no rupture even when the film was expanded up to about 4 times stretching from the original dimension (Fig. 3). The elastic coefficient of the adhered film (1.2×10^7 Pa) was found to decrease to about two-thirds of that of the untreated micropored film. The covered stent was mounted on a PTA balloon catheter [Fig. 4(a)]. The covered stent was dilated by expanding a balloon with pressurized water [Fig. 4(b)]. After balloon deflation and subsequent removal of the balloon catheter, the shape of the stent was enough maintained without shrinkage [Fig. 4(c)]. As a model device for implantation, a half-covered stent was prepared by wrapping half of the outer surface of the stent strut with the heparin-loaded gelatin-layered SPU film similarly to the fully covered stent as mentioned above [Fig. 2(b)].

Implantation and histological evaluation

The half-covered stent, with the covered area on the distal side, was mounted in a PTA balloon-expandable

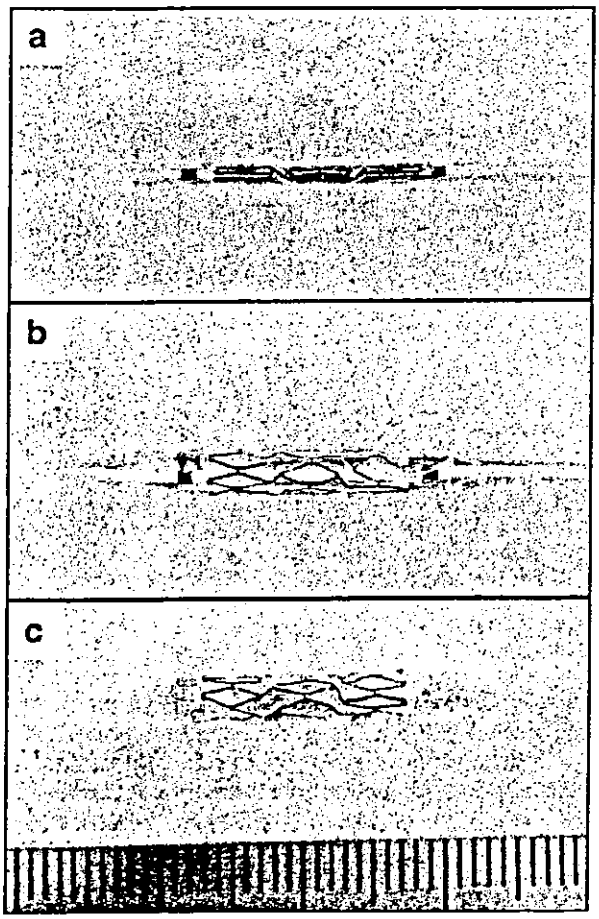

Figure 4. Gross appearance of the covered stent after mounting on a PTA balloon catheter (a), after dilation by expansion of the balloon (b), and after deflation and removal of the balloon (c).

catheter, and inserted from the femoral artery through a 5F sheath introducer, taking care not to slip both the stent and the cover film out of the balloon. The covered stents could be smoothly manipulated in blood vessels, and no differences in handling were noted irrespective of the presence of covering. The stent was navigated into the common carotid artery under fluoroscopy and placed by dilation of the PTA balloon. There was no difference in the dilation of the stent with or without covering.

Angiography immediately after implantation showed that all arteries (n = 7) were patent with no sign of intraluminal defects. In addition, angiography after 3-month implantation showed that all stents were patent. No significant intimal hyperplasia was macroscopically observed in the stent [Fig. 5(a)]. SEM observation indicated that the surface of the stent was covered with confluent endothelial cells in all cases, irrespective of covered or noncovered region (Fig. 6). The endothelial cells in all luminal surfaces exhibited a normal spindle shape and the direction of cellular elongation paralleled that of blood flow. This resembled the typical morphologic features of endothelial cells in natural vessels. Genesis of thin neointimal layers was observed around the strut in the noncovered stent region shown in the cross-section of the implanted sample [Fig. 5(b)]. In the covered region, thin neointimal layers were observed mainly on the surface of the film lumen, and the neogenetic and old intimal layers were united through the micropores produced on the film [Fig. 5(c)]. There was little difference in the neointimal layers between covered and noncovered regions. The mean thickness of the neointimal layers was 230.6 ± 57.5 μm in the uncovered region and 244.3 ± 48.5 μm including cover film thickness in the covered region.

DISCUSSION

For the treatment of arteriosclerotic stenosis lesions, stent angioplasty, which is much less invasive than the conventional surgical treatment, has widely been performed.[3–6] However, 25 ~ 30% of restenosis rates observed in a few months after stenting have been reported, which remains an unsolved problem. To reduce the restenosis rate as much as possible, various "second-generation" stents have been under development by incorporation of various working principles including surface designs such as polymer coating or fixation[19,39–46] and immobilization of pharmacological agents,[14–29] material designs such as metallic[47,48] for biocompatibility, and biodegradability and architectural design for flexibility and resistance against recoiling, as mentioned below.

The polymer materials used in these studies were degradable polymers such as polyglycolic acid[43] and polylactic acid[42–44] or nondegradable polymers such as polyurethane,[39,40] silicon,[46] and polyester.[41] However, it has been reported that stents covered with non-pored-polymer films implanted in the swine coronary artery caused significant inflammation, thrombus formation, and an excessive growth of SMCs, resulting in severe stenosis. This is because a covering film greatly increases the blood-contact surface area, which eventually increases the frequency of thrombus formation and inflammatory reaction. Therefore, a

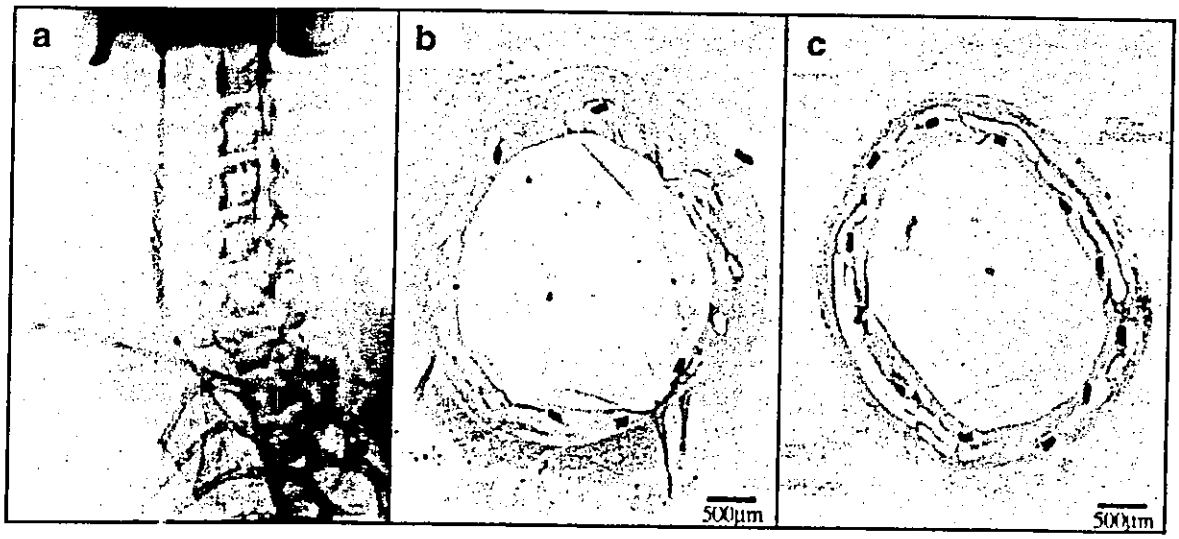

Figure 5. Angiograph of the rabbit common carotid artery after 3-month implantation of the half-covered stent (a). Light micrographs of the circumferential sections of the rabbit common carotid arteries implanted with the half-covered stent (c); bared region (b); and covered region (c) in the stent.

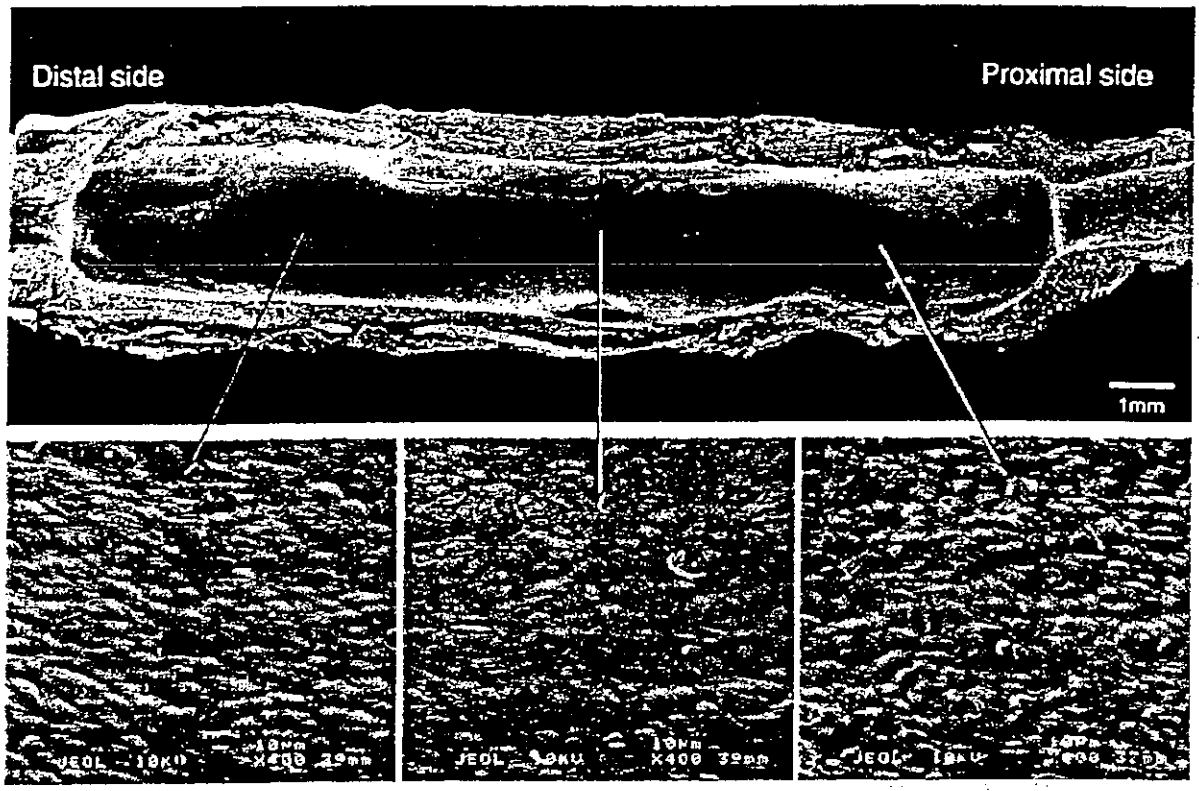

Figure 6. SEM of the luminal surface of the rabbit common carotid artery implanted with the half-covered stent.

high degree of anti-coagulation, minimal inflammation, and rapid endothelialization are essential properties for a "covered" stent. The first of these can be realized by heparin release from a gelatin gel-layered surface, the second may be achieved by using a nonbiodegradable biocompatible surface, and the last is mainly achieved by controlling the transmural tissue ingrowth of accompanying capillaries. Thus, microporosity is an essential factor for improved endothelialization and arterial tissue regeneration similar to the results observed for small-diameter artificial grafts[35,36] as well as a model "covered" stent in our previous study: SPU film-wrapped stents with regionally different pore densities in the circumferential configuration differentiated in the degree of tissue ingrowth, which depends on the pore density.[8]

In this study, we newly designed and devised a covered stent with the dual functions of drug reservoir/release and physical control of tissue ingrowth. Such a covering material should: 1. be a durable thin elastomeric film (which minimally increases the diameter of the stent because the diameter of diseased coronaries is approximately 3 mm, and that of stents in the nonexpanded state is approximately 1 ~ 1.5 mm but in the expanded state is approximately 3 mm). This means that approximately two- to three-fold stretching of the covered film occurred in the circumferential direction upon expansion; 2. be micropored with high-dimensional precision and at a well-defined pore density; and 3. provide a drug-loading matrix on both faces of the film surface. A drug-loaded covered film contacts with a much larger tissue area than a drug-loaded strut. SPU film was selected because it satisfies the requirements mentioned above in terms of durability, elasticity, high-quality microporing, and surface modification. Our previous article showed that precision processing of micropores at micron levels can be achieved using an ablation process with a pulsed excimer laser which has high energy in the UV region.[37,49] Multiple microporing, which is manipulated by computer-assisted design, reduced the elastic coefficient of the film (Fig. 3). The assembled covered stent could be easily expanded by inflation of an inserted balloon, in the same way as a noncovered stent. As the surface-layered drug-reservoir matrix, benzophenone-derivatized gelatin,[32] which was previously used for fabrication of SPU film-based small-diameter artificial grafts,[35,36] served effectively in stent application. Upon UV irradiation, radicals generated by photolysis of benzophenone groups lead to photocrosslinking between gelatin molecules as well as surface covalent bonding. Anti-coagulation was attained by impregnation of heparin in the photocured gelatin layer fixed on the SPU film. At 3-month implantation, all stents

were patent without significant intimal hyperplasia: there was little difference in the intimal thickness between the noncovered and covered regions of the "half-covered" stents, indicating that the immobilized and/or released heparin on the blood-contacting surface of the cover film effectively suppressed or minimized thrombus formation. Sooner or later, complete endothelialization on the struts of the stent and cover film appeared to proceed (Fig. 6). This was attributed to tissue ingrowth from both ends of the covered film as well as through the micropores [Fig. 5(b, c)], and indicates that, despite the presence of a foreign material, micropored SPU film did not significantly trigger the foreign body reactions that usually lead to excessive tissue ingrowth.

In this study, only the luminal surface (or blood-contacting face of film) was immobilized with heparin, simply focusing on anti-coagulation at the blood-contacting surface. However, drug loading on the tissue-facing surface may alter the morphogenesis process at atherosclerotic sites, reverting them to the normal tissue architecture if an appropriate drug is selected. Such candidate drugs may exert pharmacological or biological actions on cell proliferation, cell-cycle arrest, apoptosis, and/or phenotypic reversion of SMCs from "synthetic" to "contractile" type. That is, synthetic-phenotype SMCs, which exist in atherosclerotic sites, are highly proliferative and massively produce extracellular matrix components, both of which are major causes of intimal hyperplasia, whereas contractile-phenotype SMCs are in the quiescent state of their cell cycle—a phase of no-proliferation and no extracellular matrix synthesis, as is found in normal vascular tissue.[50,51]

In addition to suppressed intimal hyperplasia via sustained release from the matrix on the tissue-facing surface, the micropored film may act as a physical barrier controlling tissue ingrowth on the blood-contacting surface face in two manners. As shown in Figure 5c, vascular-type cells migrated from the tissue to the blood-contacting surface through micropores, resulting in neointimal tissue formation and subsequent endothelialization. Rapid endothelialization is the ultimate good for control of normal tissue regeneration. Our previous *in vitro*[49] and *in vivo*[8] studies revealed that optimal microporing is essentially needed for the control of cell migration from one side of the film surface to the other side, and that pore size and pore density are the real determinants for cellular migration and tissue ingrowth. As exemplified with other researchers' studies, nonpermeable films do not form neointimal tissue. Therefore, the high risk of continuous occurrence of thrombus is not circumvented in nature.

The other possible effect of a cover film on morphogenesis is to serve as a protective membrane resistant to "recoil" phenomena in the chronic phase,[52,53] in which SMCs which have accumulated in neointimal tissue and are highly elongated circumferentially self-contract to fasten the vessel wall: this generates inward tissue pressure, reducing the luminal diameter of a vessel. This recoiling often occurs after a prolonged period of implantation. The "protective or barrier membrane" may physically inhibit the "recoil" phenomena, whereas the minimally micropored area provides capillary-accompanying tissue ingrowth, resulting in endothelialization. Thus, by the concerted actions of sustained release of bioactive substances [for example, anti-coagulant (or heparin),[23–27] anti-proliferative agents (heparin for SMCs or anti-cancer agent[15,16,21,22] or cell-cycle modifier[28,29]), angiogenesis-inducing growth factor (or vascular endothelial growth factor)], and a physical barrier as mentioned above, intimal hyperplasia and mechanical recoiling may be prevented. This is our hypothetical appraisal of the "covered" stent and its potential performance in clinical situations.

To validate this hypothesis, we are now evaluating the usefulness of "full covered" stents using an animal model under conditions more directly resembling clinical applications: rabbits with hyperlipidemia and an intimal hypertrophy produced by balloon-induced denudation of endothelium are being used as an atherosclerotic animal model. The results for up to 7-month implantation will be reported in the near future.

References

1. Gruntzig AR, Senning A, Siegenthaler WE. Nonoperative dilation of coronary-artery stenosis: Percutaneous transluminal coronary angioplasty. N Engl J Med 1979;301:61–68.
2. Lee G, Ikeda RM, Joye JA, Bogren HG, DeMaria AN, Mason DT. Evaluation of transluminal angioplasty of chronic coronary artery stenosis: Value and limitations assessed in fresh human cadaver hearts. Circulation 1980;61:77–83.
3. Sigwart U, Puel J, Mirkovitch V, Joffre F, Kappenberger L. Intervascular stents to prevent occlusion and restenosis after transluminal angioplasty. N Engl J Med 1987;316:701–706.
4. Serruys PW, de Jaegere P, Kiemeneij F, Macaya C, Rutsch W, Heyndrickx G, Emanuelsson H, Marco J, Legrand V, Materne P, Belardi J, Sigwart U, Colombo A, Goy JJ, van der Heuvel P, Delcan J, Morel MA. A comparison of balloon-expandable-stent implantation with balloon angioplasty in patients with coronary artery disease. N Engl J Med 1994;331:489–495.
5. Fiscman DL, Leon MB, Baim DS, Schatz RA, Savage MP, Penn I, Detre K, Veltri L, Ricci D, Nobuyoshi M, Cleman M, Heuser R, Almond D, Teirstein PS, Fish RD, Colombo A, Brinker J, Moses J, Shaknovich A, Hirshfeld J, Bailey S, Ellis S, Rake R, Goldberg S. A randomized comparison of coronary-stent placement and balloon angioplasty in the treatment of coronary artery disease. N Engl J Med 1994;331:496–501.
6. Erbel R, Haude M, Hopp HW, Franzen D, Rupprecht HJ, Heublein B, Fisher K, de Jaegere P, Serruys P, Rutsch W, Probst P. Coronary-artery stenting compared with balloon angioplasty for restenosis after intimal balloon angioplasty. N Engl J Med 1998;339:1672–1678.

7. Van der Giessen WJ, Licoff AM, Schwartz RS, van Beusekom HM, Serruys PW, Holmes DR Jr, Ellis SG, Topol EJ. Marked inflammatory sequelae to implantation of biodegradable and nonbiodegradab e polymers in porcine coronary arteries. Circulation 1996;94:1690–1697.
8. Nakayama Y, Nishi S, Ishibashi-Ueda H, Matsuda T. Surface microarchitectural design in biomedical applications: *In vivo* analysis of tissue ingrowth in excimer laser-directed micropored scaffold for cardiovascular tissue engineering. J Biomed Mater Res 2000;51:520–528.
9. Uematsu M, Okada M. Self-expandable vascular stent covered with polyurethane membrane: An experimental preliminary study of a placement in the thoracic descending aorta of a rabbit using endovascular intervention. Ann Thorac Cardiovasc Surg 2000;6:137–141.
10. McKenna CJ, Camrud AR, Sangiorgi G, Kwon HM, Edwards WD, Holmes DR Jr, Schwartz RS. Fibrin-film stenting in a porcine coronary injury model: Efficacy and safety compared with uncoated stents. J Am Coll Cardiol 1998;31:1434–1438.
11. De Scheerder I, Szilard M, Yanming H, Ping XB, Verbeken E, Neerinck D, Demeyere E, Coppens W, Van de Werf F. Evaluation of the biocompatibility of two new diamond-like stent coatings (Dylyn) in a porcine coronary stent model. J Invasive Cardiol 2000;12:389–394.
12. Whelan DM, van der Giessen WJ, Krabbendam SC, van Vliet EA, Verdouw PD, Serruys PW, van Beusekom HM. Biocompatibility of phosphorylcholine coated stents in normal porcine coronary arteries. Heart 2000;83:338–345.
13. Bertrand OF, Sipehia R, Mongrain R, Rodes J, Tardif JC, Bilodeau L, Cote G, Bourassa MG. Biocompatibility aspects of new stent technology. J Am Coll Cardiol 1998;32:562–571.
14. Lahann J, Klee D, Pluester W, Hoecker H. Bioactive immobilization of γ-hirudin on CVD-coated metallic implant devices. Biomaterials 2001;22:817–826.
15. de Smet BJ, de Kleijn D, Hanemaaijer R, Verheijen JH, Robertus L, van Der Helm YJ, Borst C, Post MJ. Metalloproteinase inhibition reduces constrictive arterial remodeling after balloon angioplasty: A study in the atherosclerotic Yucatan micropig. Circulation 2000;101:2962–2967.
16. Cherr GS, Motew SJ, Travis JA, Fingerle J, Fisher L, Brandl M, Williams JK, Geary RL. Metalloproteinase inhibition and the response to angioplasty and stenting in atherosclerotic primates. Arterioscler Thromb Vasc Biol 2002;22:161–166.
17. Lincoff AM, Furst JG, Ellis SG, Tuch RJ, Topol EJ. Sustained local delivery of dexamethasone by a novel intravascular eluting stent to prevent restenosis in the porcine coronary injury model. J Am Coll Cardiol 1997;29:808–816.
18. Yamawaki T, Shimokawa H, Kozai T, Miyata K, Higo T, Tanaka E, Egashira K, Shiraishi T, Tamai H, Igaki K, Takrshita A. Intramural delivery of a specific tyrosine kinase inhibitor with biodegradable stent suppresses the restenotic changes of the coronary artery in pigs *in vivo*. J Am Coll Cardiol 1998;32: 780–786.
19. Nakayama Y, Ji-Youn K, Nishi S, Ueno H, Matsuda T. Development of high-performance stent: Gelatinous photogel-coated stent that permits drug delivery and gene transfer. J Biomed Mater Res 2001;57:559–566.
20. Lambert TL, Dev V, Rechavia E, Forrester JS, Litvack F, Eigler NL. Localized arterial wall drug delivery from a polymer-coated removable metallic stent: Kinetics, distribution, and bioactivity of forskolin. Circulation 1994;90:1003–1011.
21. Farb A, Heller PF, Shroff S, Cheng L, Kolodgie FD, Carter AJ, Scott DS, Froehlich J, Virmani R. Pathological analysis of local delivery of paclitaxel via a polymer-coated stent. Circulation 2001;104:473–479.
22. Heldman AW, Cheng L, Jenkins GM, Heller PF, Kim DW, Ware M Jr, Nater C, Hruban RH, Rezai B, Abella BS, Bunge KE, Kinsella JL, Sollott SJ, Lakatta EG, Brinker JA, Hunter WL, Froehlich JP. Paclitaxel stent coating inhibits neointimal hyperplasia at 4 weeks in a porcine model of coronary restenosis. Circulation 2001;103:2289–2295.
23. Hardhammar PA, van Beusekom HMM, Emanuelsson HU, Hofma SH, Albertsson PA, Verdouw PD, Boersma E, Serruys PW, van der Giessen WJ. Reduction in thrombotic events with heparin-coated Palmaz-Schatz stents in normal porcine coronary arteries. Circulation 1996;93:423–430.
24. Blezer R, Cahalan L, Cahalan PT, Lindhout T. Heparin coating of tantalum coronary stents reduces surface thrombin generation but not factor Xa generation. Blood Coagul Fibrinolysis 1998;9:435–440.
25. van Der Giessen WJ, van Beusekom HM, Larsson R, Serruys P. Heparin-coated coronary stents. Curr Interv Cardiol Rep 1999; 1:234–240.
26. Beythien C, Gutensohn K, Bau J, Hamm CW, Kuhnl P, Meinertz T, Terres W. Influence of stent length and heparin coating on platelet activation: A flow cytometric analysis in a pulsed floating model. Thromb Res 1999;94:79–86.
27. Vrolix MC, Legrand VM, Reiber JH, Grollier G, Schalij MJ, Brunel P, Martinez-Elbal L, Gomez-Recio M, Bar FW, Bertrand ME, Colombo A, Brachman J. Heparin-coated Wiktor stents in human coronary arteries (MENTOR trial). MENTOR Trial Investigators. Am J Cardiol 2000;86:385–389.
28. Sousa JE, Costa MA, Abizaid AC, Rensing BJ, Abizaid AS, Tanajura LF, Kozuma K, Van Langenhove G, Sousa AG, Falotico R, Jaeger J, Popma JJ, Serruys PW. Sustained suppression of neointimal proliferation by sirolimus-eluting stents: One-year angiographic and intravascular ultrasound follow-up. Circulation 2001;104:2007–2011.
29. Sousa JE, Costa MA, Abizaid A, Abizaid AS, Feres F, Pinto IM, Seixas AC, Staico R, Mattos LA, Sousa AG, Falotico R, Jaeger J, Popma JJ, Serruys PW. Lack of neointimal proliferation after implantation of Sirolimus-coated stents in human coronary arteries: A quantitative coronary angiography and three-dimensional intravascular ultrasound study. Circulation 2001; 103:192–195.
30. Jawien A, Bowen-Pope DF, Libdner V, Schwartz SM, Clowes AW. Platelet-derived growth factor promotes smooth muscle migration and intimal thickening in a rat model of balloon angioplasty. J Clin Invest 1992;89:507–511.
31. Pitsch RJ, Minion DJ, Goman ML, van Aalst JA, Fox PL, Graham LM. Platelet-derived growth factor production by cells from Dacron grafts implanted in a canine model. J Vasc Surg 1997;26:70–78.
32. Nakayama Y, Okuda K, Matsuda T. Preparation of multifunctional gelatin or albumin-based macromors and visible light-induced gelation of these aqueous solutions. Biomacromolecules. Submitted for publication.
33. Okino H, Nakayama Y, Tanaka M, Matsuda T. *In situ* hydrogelation of photocurable gelatin and drug release. J Biomed Mater Res 2002;59:233–245.
34. Nakayama Y, Matsuda T. Photocurable surgical tissue adhesive glues composed of photorective gelatin and poly(ethylene glycol) diacrylate. J Biomed Mater Res 1999;48:511–521.
35. Doi K, Nakayama Y, Matsuda T. Novel compliant and tissue-permeable microporous polyurethane vascular prosthesis fabricated using an excimer laser ablation technique. J Biomed Mater Res 1996;31:27–33.
36. Doi K, Matsuda T. Significance of porosity and compliance of microporous, polyurethane-based microarterial vessel on neoarterial wall regeneration. J Biomed Mater Res 1997;37:573–584.
37. Nakayama Y, Matsuda T. Surface microarchitectural design in biomedical applications: Preparation of microporous polymer surfaces by an excimer laser ablation technique. J Biomed Mater Res 1995;29:1295–1301.
38. Smith PK, Mallia AK, Mermanson GT. Colorimetric method

for the assay of heparin content in immobilized heparin preparations. Anal Biochem 1980;109:466–473.
39. Holmes DR, Camrud AR, Jorgenson MA, Edwards WD, Schwartz RS. Polymeric stenting in the porcine coronary artery model: Differential outcome of exogenous fibrin sleeves versus polyurethane-coated stents. J Am Coll Cardiol 1994;24:525–531.
40. Severini A, Mantero S, Tanzi MC, Cigada A, Salvetti M, Cozzi G, Motta A. Polyurethane-coated, self-expandable biliary stent: An experimental study. Acad Radiol 1995;2:1078–1081.
41. Castaneda F, Ball SM, Wyffels PL, Young K, Li R. Assessment of a polyester-covered nitinol stent in an atherosclerotic swine model. J Vasc Interv Radiol 2000;11:483–491.
42. Schellhammer F, Berlis A, Bloss H, Pagenstecher A, Schumacher M. Poly-lactic-acid coating for endovascular stents: Preliminary results in canine experimental arteriovenous fistulae. Invest Radiol 1997;32:180–186.
43. Hietala EM, Salminen US, Stahls A, Valimaa T, Maasilta P, Tormala P, Nieminen MS, Harjula AL. Biodegradation of the copolymeric polylactide stent: Long-term follow-up in a rabbit aorta model. J Vasc Res 2001;38:361–369.
44. Tamai H, Igaki K, Kyo E, Kosuga K, Kawashima A, Matsui S, Komori H, Tsuji T, Motohara S, Uehata H. Initial and 6-month results of biodegradable poly-L-lactic acid coronary stents in humans. Circulation 2000;102:399–404.
45. Petas A, Vuopio-Varkila J, Siitonen A, Valimaa T, Talja M, Taari K. Bacterial adherence to self-reinforced polyglycolic acid and self-reinforced polylactic acid 96 urological spiral stents *in vitro*. Biomaterials 1998;19:677–681.
46. Ozbek C, Heisel A, Gross B, Bay W, Schieffer H. Coronary implantation of silicone-carbide-coated Palmaz-Schatz stents in patients with high risk of stent thrombosis without oral anticoagulation. Cathet Cardiovasc Diagn 1997;41:71–78.
47. Kastrati A, Schomig A, Dirschinger J, Mehilli J, von Welser N, Pache J, Schuhlen H, Schilling T, Schmitt C, Neumann FJ. Increased risk of restenosis after placement of gold-coated stents: Results of a randomized trial comparing gold-coated with uncoated steel stents in patients with coronary artery disease. Circulation 2000;30:2478–2483.
48. Edelman ER, Seifert P, Groothuis A, Morss A, Bornstein D, Rogers C. Gold-coated NIR stents in porcine coronary arteries. Circulation 2001;103:429–434.
49. Matsuda T, Nakayama Y. Surface microarchitectural design in biomedical applications: *In vitro* transmural endothelialization on microporous segmented polyurethane films fabricated using an excimer laser. J Biomed Mater Res 1996;31:243–249.
50. Neuville P, Yan Z, Gidlof A, Pepper MS, Hansson GK, Gabbiani G, Sirsjo A. Retinoic acid regulates arterial smooth muscle cell proliferation and phenotypic features *in vivo* and *in vitro* through an RARalpha-dependent signaling pathway. Arterioscler Thromb Vasc Biol 1999;19:1430–1436.
51. Kocher O, Gabbiani F, Gabbiani G, Reidy MA, Cokay MS, Peters H, Huttner I. Phenotypic features of smooth muscle cells during the evolution of experimental carotid artery intimal thickening: Biochemical and morphologic studies. Lab Invest 1991;65:459–470.
52. Chan AW, Moliterno DJ. In-stent restenosis: Update on intracoronary radiotherapy. Cleve Clin J Med 2001;68:796–803.
53. Mintz GS. Remodeling and restenosis: Observations from serial intravascular ultrasound studies. Curr Interv Cardiol Rep 2000;2:316–325.

ELSEVIER

Cardiovascular Radiation Medicine 4 (2003) 77–82

CARDIOVASCULAR RADIATION MEDICINE

Fabrication of drug-eluting covered stents with micropores and differential coating of heparin and FK506

Yasuhide Nakayama[a,*], Shogo Nishi[b], Hatsue Ishibashi-Ueda[c]

[a]*Department of Bioengineering, National Cardiovascular Center Research Institute, Fujishiro-dai 5-7-1, Suita, Osaka 565-8565, Japan*
[b]*Department of Neurosurgery, Takatsuki Red Cross Hospital, Abuno 1-1-1, Takatsuki, Osaka 569-1096, Japan*
[c]*Department of Pathology, National Cardiovascular Center Hospital, Fujishiro-dai 5-7-1, Suita, Osaka 565-8565, Japan*

Received 28 May 2003; accepted 30 May 2003

Abstract To reduce in-stent restenosis rates, we developed a novel drug-eluting covered stent with a microporous elastometric covered film, in which its luminal surface was flat and immobilized with heparin for anticoagulation and its outer surface immobilized with FK506 to prevent neointimal hyperplasia. One month after implantation into the bilateral common carotid arteries, all stented arteries were patent and the luminal surfaces were fully covered with a confluent of endothelial cells irrespective of the drug immobilization. In the control group, which consisted of covered stents without drug immobilization, intensive inflammatory cells adjacent to the stents and neointimal hyperplasia, indicating vascular injury, were observed. In contrast, in the developed drug-eluting stents, only a few inflammatory cells around the stent strut and covered film were observed, and there was no significant neointimal thickening.

Keywords: Stents; Drug-eluting; Covered stents; Micropore; FK506; Heparin

1. Introduction

Percutaneous transluminal angioplasty in coronary and peripheral arteries (PTCA or PTA) using either balloon catheters or metallic stents has been widely used for the clinical treatment of atheroscleotic stenosis [1–6]. Due to the reduced incidence of restenosis derived from excessive tissue in-growth, endovascular metallic stenting has become more popular than balloon angioplasty. However, it has been reported that a few months after stenting, restenosis rates of 25–30% occur, which remains an unsolved problem.

To reduce the in-stent restenosis rate, we attempted to produce covered stents, in which a covering of an elastomeric film was loaded over a stent strut to provide a physical barrier against tissue in-growth [7,8]. This film should also be expected to serve as a pharmacological reservoir for delivery of drugs. As the first step, a covered stent with a wrapping of microporous elastomeric film over a stent strut was designed, with the strut placed at the inner side of the film.

In this study, we developed a novel drug-eluting covered stent as a modification of the previously prepared covered stent. The structural design of the covered stent is shown in Fig. 1. The stent strut was buried into a cover film, which provided a flat luminal surface for improved reliability of the anticoagulation. In addition, the cover film was differentially coated with two alternative drugs to satisfy an appropriate requirement for each surface; that is, its luminal surface was immobilized with heparin for anticoagulation, and the outer surface was immobilized with FK506 (tacrolims) [9,10] for the prevention of neointimal hyperplasia. Firstly, a fabrication method for the covered stents is described, and, subsequently, the covered stents were implanted into common carotid arteries of rabbits as a preliminary experiment.

2. Experimental

2.1. Preparation of covered stents

A tetrahydrofuran solution containing 5 wt.% of segmented polyurethane (SPU; Miractran Japan, Kanagawa,

* Corresponding author. Tel.: +81-6-6833-5012; fax: +81-6-6872-8090.
E-mail address: nakayama@ri.ncvc.go.jp (Y. Nakayama).

1522-1865/03/$ – see front matter © 2003 Elsevier Inc. All rights reserved.
doi:10.1016/S1522-1865(03)00143-4

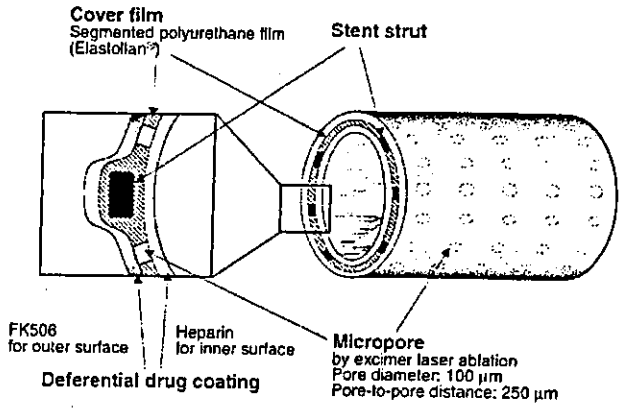

Fig. 1. The structural design of the developed covered stent. The stent strut is buried into the cover film and the luminal surface is flat. The cover film was micropored (pore diameter; 100 μm and pore-to-pore distance; 250 μm) and coated with a photogelated gelatin, immobilized with heparin on the inner surface and FK506 in the outer surface.

Japan) was dip-coated on a stainless-steel rod (2 mm in diameter, 100 mm in length) up to 50 mm from the end and was air-dried. After repeating the procedure twice, a SPU tube with a thickness of around 20 μm was formed on the rod. The SPU-coated rod was mounted at the center of the SPU-coated region with a Palmaz–Schatz stent (Johnson & Johnson Medical Japan, Tokyo, Japan), predilated to 25 mm in diameter, and over-dip-coated three times with the SPU solution. The total thickness of the SPU film was around 50 μm. The rod coated with the SPU film buried with the stent was micropored using a KrF excimer laser apparatus [11] (L4500; Hamamatsu Photonics, Shizuoka, Japan). The pore diameter was fixed at 100 μm, and the pore-to-pore distance was fixed at 200 μm. After completion of micro-processing, the rod was removed to obtain a microporous SPU-covered stent. The inner and outer surfaces of the cover film were coated with an aqueous solution (40 μl/cm^2) of photoreactive gelatin [12] (5 wt.%) mixed with heparin (2.5 wt.%) or FK506 (140 μg/cm^2), respectively. Both surfaces were irradiated with a 200-W mercury–xenon arc lamp (L2859-01; Hamamatsu Photonics) for 1 min.

2.2. Implantation

The experimental animals were New Zealand white rabbits, weighing 3–4 kg. The investigations were performed according to the 'Principles of Laboratory Animal Care' (formulated by the National Society for Medical Research) and the 'Guide for the Care and Use of Laboratory Animals' (National Institutes of Health Publication, No. 56-23, revised 1985). Heparin (2000 IU) was administered only during angiography. The covered stent mounted on a PTA balloon catheter (3.0 mm, 2 cm, SAVVY, Johnson & Johnson) was positioned into the common carotid artery (approximately 3 mm) from the femoral artery through a 5F sheath introducer under fluoroscopy using a standard PTCA micro-guide wire. The balloon was inflated at a pressure of 8 atm for 30 s, deflated and then slowly withdrawn, leaving the covered stent in place. Neither antiplatelet agents nor additional anticoagulants were administered during the 1-month follow-up period.

2.3. Microscopic examination

One month after stenting, animals were anesthetized, and a preeuthanasia angiogram of the common carotid arteries was conducted, followed by euthanasia and perfusion–fixation. The stented arteries were dissected free and fixed with 10% formaldehyde in phosphate buffer (pH 7.4) for over 48 h prior to light microscopy and scanning electron microscopy (SEM). Specimens for light microscopy were dehydrated with an alcohol series and embedded in glycolmethacrylate. Thin sections of the tissues were prepared in the direction of the circumference, subjected to standard hematoxylin and eosin staining, and then observed under a light microscope (E1000M; Nikon, Tokyo, Japan). Specimens for SEM were postfixed with 1% osmium tetraoxide, dehydrated in a graded series of ethanol, critical point dried and then sputter-coated with platinum. The surfaces of longitudinally cut stents were observed using a SEM (JSM-6301; JEOL, Tokyo, Japan).

3. Results

3.1. Fabrication of covered stent

The covered stent was prepared according to the procedure as shown in Fig. 2. At first, a tubular film of SPU was prepared on the outer surface of a stainless-steel rod following a repetition cycle of immersion into a SPU solution and then drying (Step I). After mounting with a commercially available balloon-expandable stent (Step II), the SPU film-coated rod was overcoated with a SPU film using the same procedure as mentioned above (Step III).

Subsequently, the SPU film was micropored using a previously developed excimer laser ablation technique [11] (Step IV). Irradiation of pulsed UV light from the excimer laser processing apparatus through a photomask with a round aperture of 2.2 mm in diameter produced a micropattern of micropores of 100 μm in diameter, with an interpore distance of 200 μm. After removal from the stainless-steel rod, the covered stent with a microporous SPU film was obtained (Step V). Because the stent strut was interposed into the SPU cover film, the inner surface of the covered stent was flat.

Finally, the inner and outer surface of the cover film were coated with either a mixed aqueous solution of photoreactive gelatin and heparin or a mixed aqueous solution of photoreactive gelatin [12] and FK506 and were subsequently irradiated with UV light for drug immobilization onto a thin layer of photoproduced gelatinous hydrogel, which was

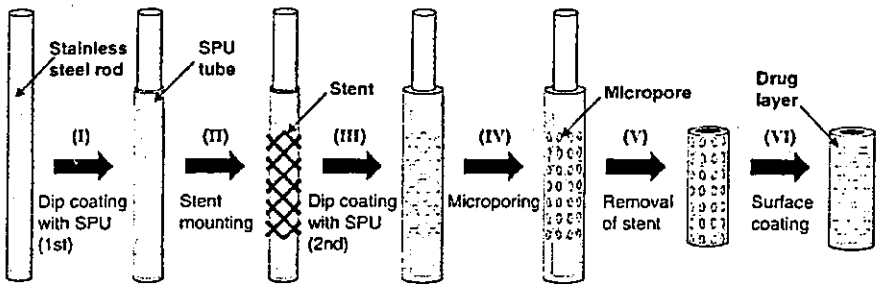

Fig. 2. A schematic diagram of the preparation of the covered stent. A stainless-steel rod was firstly dipped into a SPU solution to fabricate a SPU tube around the rod (I), this was followed by mounting of the balloon-expandable stent on the SPU-coated rod (II) and overcoating the stent-mounted rod with the SPU solution using a dipping process (III). Thereafter, microporing the SPU film with ablation using an excimer laser was performed (IV), followed by removal of the covered stent from the rod (V) and finally coating the surface with a drug using a photoreactive gelatin by UV irradiation (heparin for the inner surface and FK506 for the outer surface) (VI).

chemically fixed on both sides of the SPU cover film (Step VI).

The drug-immobilized microporous covered stent was then mounted on a commercially available PTA balloon-expandable catheter. Using this procedure, no rupturing occurred, even when the covered stent was dilated up to 3 mm in diameter by expanding the balloon with pressurized water (Fig. 3A and B). No differences in dilation of the stent were noted irrespective of the presence of covering. After balloon deflation and subsequent removal of the balloon catheter, the stent maintained its shape with no shrinkage.

3.2. *In vivo performance*

The covered stent, mounted on a PTA balloon-expandable catheter, was inserted into the femoral artery through a 5F sheath introducer, taking precaution not to slip both the stent and the cover film out of the balloon. The covered stents could be smoothly manipulated in the blood vessels, and no differences in handling were noted irrespective of the presence of the covering. The stent was navigated into the bilateral common carotid arteries of rabbits under fluoroscopy and placed by dilating the PTA balloon (Fig. 3C). As a control, stents covered with a microporous film but no drug coating were used.

Immediately after implantation, all arteries were patent with no sign of intraluminal defects regardless of the presence or absence of a drug coating. The presence of FK506 in blood was still observed after 3 days of deployment (32.4 ng/ml immediately after deployment and 4.2 ng/ml after 3 days of deployment). One month after implantation, angiographs of all the stents showed patent with no significant intimal hyperplasia. In addition, SEM observation indicated that the surfaces of the stents were fully covered with a confluent of endothelial cells, irrespective of the drug coating (Fig. 3D). The endothelial cells in all the luminal surfaces exhibited a normal spindle shape and the direction of cellular elongation paralleled that of the blood flow. Histological evaluation showed that in the control group, intensive inflammatory cells adjacent to the stents and neointimal hyperplasia, indicating vascular injury, were observed (Fig. 3E). In contrast, in the drug-eluting stents, few inflammatory cells around the stent strut, and no significant neointimal thickening, were observed (Fig. 3F). The mean thickness of the neointimal

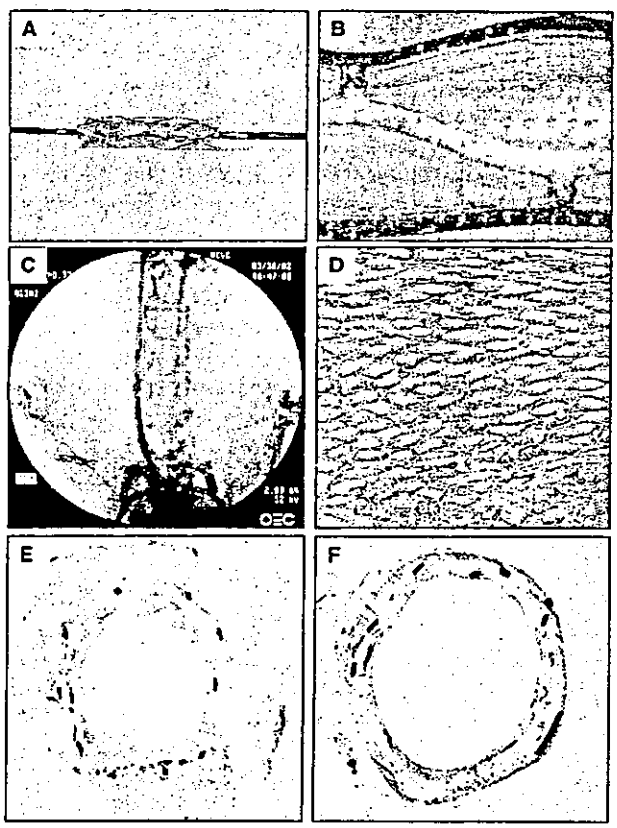

Fig. 3. (A and B) Gross appearance of the covered stent after dilation by expansion of a PTA balloon catheter. Angiograph (C) and SEM photo (D) of the rabbit common carotid artery 1 month after implantation of the covered stent. Light micrographs of circumference sections of the rabbit common carotid arteries 1 month after implantation of the covered stents either without (E) or with (F) drug immobilization.

layer and percentage of stenosis area were ca. 120 μm and ca. 25%, respectively, both of which were less than half the level of the control group.

4. Discussion

To reduce restenosis rates, high-performance stents are being developed, which incorporate various working principles, including surface designs such as coating or immobilization of pharmacological agents [13–24], material designs such as metallic [25,26] or polymers [27–35] for biocompatibility or biodegradability and shape designs for flexibility [36,37]. In particular, drug-eluting stents are expected to cause a revolutionary change. Indeed, recent clinical trials have shown that stents immobilized with Rapamycin (Sirolimus) or Paclitaxel can inhibit vascular smooth muscle cell proliferation and migration in vitro, and thus demonstrate their potential for the treatment of de novo lesions.

Recently, we have developed a covered stent with the dual functions of physical control of tissue in-growth in stents and drug reservoir/release [7,8]. In our previous study [7,8], the first model of the covered stent was fabricated by wrapping a micropored elastomeric film over a stent followed by suturing and gluing. However, there were two major problems in this fabrication method for the covered stent.

The first problem concerned the geometrical structure of the luminal surface of the stent. Because the cover film was wrapped over the outer side of the strut, the strut was placed at the luminal surface of the cover film. Such an uneven structure of the luminal surface may trigger thrombus formation immediately after implantation. Large amounts of thrombus may lead to occlusion of the stented arteries. In addition, platelet-derived growth factor (PDGF), secreted from aggregated platelets in the thrombus, is a potent mitogenic substance for smooth muscle cells, which is one of the principal cells triggering intimal hyperplasia. In our previous paper [7], histological examination of arteries implanted with this type of wrapping of covered stents without heparin immobilization showed that thrombus was formed around the strut. On the other hand, in this study, the covering of the stents was performed using a dip-coating method in which the strut could be buried into the cover film. From this, the whole strut of the stent was fully covered with film and a flat luminal surface was obtained, both of which are expected to prevent blood coagulation. In practice, a little thrombus formation at the luminal surface of the cover film was observed 1 month after implantation even without heparin immobilization (Fig. 3E,F). Therefore, it was considered that PDGF-induced activation of smooth muscle cells was reduced.

The second problem involved the gluing process of the cover film during preparation of the tube. In the last process [7], when the free ends of the film were covered, they overlapped by a width of about 1 mm and then adhered by gluing with *N,N*-dimethylacrylamide. In this process, almost all of the micropores at the gluing region were clogged. Because micropores are essential for rapid endothelialization (Fig. 3D), which also guarantees anticoagulation, the lack of unclogged micropores resulted in polymer material-induced thrombus formation at an acute phase of implantation. On the other hand, with the dip-coating method, no connection process between the films was needed (Fig. 2). Therefore, a homogeneous pattern of microporing was obtained over the whole area of the cover film (Fig. 3B).

The other major property of the covered stents, in addition to providing a covering that acts as a barrier for tissue in-growth, is the possibility of differential coating of two alternative drugs on each surface of the cover film. Heparin, due to its anticoagulation properties, was selected as the drug for coating to the luminal surface (or blood-contacting face) of the cover film. However, drug loading on the tissue-facing surface may alter the morphogenesis process at atherosclerotic sites, reverting them once more to normal tissue architecture if an appropriate drug is selected. For this reason, FK506 (tacrolims) was used as a drug for the outer surface because it is known as a potent immunosuppressive agent [9,10] related to rapamycin, with its mechanism of action thought to be due to inhibition of calcineurin phosphatase. In a recent study, our data indicated that FK506 inhibited vascular smooth muscle cell migration and proliferation in a concentration-dependent manner (data not shown). In addition, FK506 has also been reported to inhibit migration of neutrophils on coated on coated vitronectin by affecting the affinity of the vitronectin receptor [38,39]. Therefore, FK506 may be an appropriate coating drug for stents. In this study, neointimal thickness was markedly reduced by two immobilized drugs. There was little correlation between mean injury score and mean neointimal thickness or percent stenosis area. However, a statistically significant proportional relationship existed in the plots of mean inflammation score, which may be dependent upon the polymer material of the cover film vs. mean neointimal thickness ($r=.98$) and percent stenosis area ($r=.83$). In the drug-eluting stents, an extremely low inflammation score was obtained and was one fifth of that in the covered stents. The antiinflammatory role of FK506 may therefore be effective in the prevention of neointimal hyperplasia.

In order to validate this hypothesis, we are now evaluating the usefulness of the covered stents using animal models under conditions that more directly resemble clinical applications; rabbits with hyperlipidemia and an intimal hypertrophy produced by balloon-induced denudation of the endothelium are being used as atherosclerotic animal models. The results 6 months after implantation will be reported in the near future.

5. Conclusion

The FK506- and heparin-eluting microporous film covered stents are effective in the prevention of neointimal

thickening with a marked suppression of inflammation at the subacute phase.

Acknowledgments

This study was supported by "Research Grants for Advanced Medical Technology," "Human Genome, Tissue Engineering and Food Biotechnology" and "Aging and Health" from the Ministry of Health, Labour and Welfare of Japan and by the Grant-in-Aid for Scientific Research (B2-13450302) from the Ministry of Education, Science, Sports and Culture of Japan.

References

[1] Gruntzig AR, Senning A, Siegenthaler WF. Nonoperative dilation of coronary-artery stenosis: percutaneous transluminal coronary angioplasty. N Engl J Med 1979;301:61–8.

[2] Lee G, Ikeda RM, Joye JA, Bogren HG, DeMaria AN, Mason DT. Evaluation of transluminal angioplasty of chronic coronary artery stenosis. Value and limitations assessed in fresh human cadaver hearts. Circulation 1980;61:77–83.

[3] Sigwart U, Puel J, Mikrovitch V, Joffre F, Kappenberger L. Intravascular stents to prevent occlusion and restenosis after transluminal angioplasty. N Engl J Med 1987;316:701–6.

[4] Serruys PW, de Jaegere P, Kiemeneij F, Macaya C, Rutsch W, Heyndrickx G, Emanuelsson H, Marco J, Legrand V, Materne P, Belardi J, Sigwart U, Colombo A, Goy JJ, van der Heuvel P, Delcan J, Morel MA. A comparison of balloon-expandable-stent implantation with balloon angioplasty in patients with coronary artery disease. N Engl J Med 1994;331:489–95.

[5] Fiseman DL, Leon MB, Baim DS, Schatz RA, Savage MP, Penn I, Detre K, Veltri L, Ricci D, Nobuyoshi M, Cleman M, Heuser R, Almond D, Teirstein PS, Fish RD, Colombo A, Brinker J, Moses J, Shaknovich A, Hirshfeld J, Bailey S, Ellis S, Rake R, Goldberg S. A randomized comparison of coronary-stent placement and balloon angioplasty in the treatment of coronary artery disease. N Engl J Med 1994;331:496–501.

[6] Erbel R, Haude M, Hopp HW, Franzen D, Rupprecht HJ, Hublein B, Fisher K, de Jaegere P, Serruys P, Rutsch W, Probst P. Coronary-artery stenting compared with balloon angioplasty for restenosis after intimal balloon angioplasty. N Engl J Med 1998;339:1672–8.

[7] Nakayama Y, Nishi S, Ueda-Ishibashi H, Matsuda T. Fabrication of micropored elastomeric film-covered stents and acute-phase performances. J Biomed Mater Res 2002;64A:52–61.

[8] Nakayama Y, Nishi S, Ishibashi-Ueda H, Matsuda T. Surface microarchitectural design in biomedical applications: in vivo analysis of tissue ingrowth in excimer laser-directed micropored scaffold for cardiovascular tissue engineering. J Biomed Mater Res 2000;51:520–8.

[9] Liu J. FK506 and cyclosporin, molecular probes for studying intracellular signal tranduction. Immunol Today 1993;14:290–5.

[10] Fruman DA, Klee CB, Bierer BE, Burakoff SJ. Calcineurin phosphatase activity in T lymphocytes is inhibited by FK 506 and cyclosporin A. Proc Natl Acad Sci U S A 1992;89:3686–90.

[11] Nakayama Y, Matsuda T. Surface microarchitectural design in biomedical applications: preparation of microporous polymer surfaces by an excimer laser ablation technique. J Biomed Mater Res 1995;29:1295–301.

[12] Nakayama Y, Matsuda T. Photocurable surgical tissue adhesive glues composed of photoreactive gelatin and poly(ethylene glycol) diacrylate. J Biomed Mater Res 1999;48:511–21.

[13] Fattori R, Piva T. Drug-eluting stents in vascular intervention. Lancet 2003;361:247–9.

[14] Lahann J, Klee D, Pluester W, Hoecker H. Bioactive immobilization of γ-hirudin on CVD-coated metallic implant devices. Biomaterials 2001;22:817–26.

[15] de Smet BJ, de Kleijn D, Hanemaaijer R, Verheijen JH, Roberus L, van Der Helm YJ, Borst C, Post MJ. Metalloproteinase inhibition reduces constrictive arterial remodeling after balloon angioplasty: a study in the atherosclerotic Yucatan micropig. Circulation 2000;101:2962–7.

[16] Cherr GS, Motew SJ, Travis JA, Fingerle J, Fisher L, Brandt M, Williams JK, Geary RL. Metalloproteinase inhibition and the response to angioplasty and stenting in atheosclerotic primates. Arterioscler Thromb Vasc Biol 2002;22:161–6.

[17] Lincoff AM, Furst JG, Ellis SG, Tuch RJ, Topol EJ. Sustained local delivery of dexamethasone by a novel intravascular eluting stent to prevent restenosis in the porcine coronary injury model. J Am Coll Cardiol 1997;29:808–16.

[18] Farb A, Heller PF, Shroff S, Cheng L, Kolodgie FD, Carter AJ, Scott DS, Froehlich J, Virmani R. Pathological analysis of local delivery of paclitaxel via a polymer-coated stent. Circulation 2001;104:473–9.

[19] Heldman AW, Cheng L, Jenkins GM, Heller PE, Kim DW, Ware M, Nater C, Hruban RH, Rezai B, Abella BS, Bunge KE, Kinsella JL, Sollott SJ, Lakatta EG, Brinker JA, Hunter WL, Froehlich JP. Paclitaxel stent coating inhibits neointimal hyperplasia at 4 weeks in a porcine model of coronary restenosis. Ciculation 2001;103:2289–95.

[20] Tanabe K, Serruys PW, Grube E, Smits PC, Selbach G, van der Giessen WJ, Staberock M, de Feyter P, Muller R, Regar E, Degerlekin N, Lighart JMR, Disco C, Backx B, Russel ME. TAXUS III trial. In-stent restenosis treated with stent-based delivery of paclitaxel incorporated in a slow-release polymer formulation. Circulation 2003;107:559–64.

[21] Hardhammar PA, van Beusekom HMM, Emanuelesson HU, Hofma SIL, Albertsson PA, Verdouw PD, Boersma E, Serruys PW, van der Giessen WJ. Reduction in thrombotic events with heparin-coated Palmaz–Schatz stents in normal porcine coronary arteries. Circulation 1996;93:423–30.

[22] van Der Giessen WJ, van Beusekom HM, Larsson R, Serruys P. Heparin-coated coronary stents. Curr Interv Cardiol Rep 1999;1:234–40.

[23] Sousa JE, Costa MA, Abizaid AC, Rensing BJ, Abizaid AS, Tanajara LF, Kozuma K, Van Langenhove G, Sousa AG, Falotico R, Jaeger J, Popma JJ, Serruys PW. Sustained suppression of neointimal proliferation by sirolimus-eluting stents: one-year angiographic and intravascular ultrasound follow-up. Circulation 2001;104:2007–11.

[24] Sousa JE, Costa MA, Abizaid A, Abizaid AS, Feres F, Pinto IM, Seixas AC, Staico R, Mattos LA, Sousa AG, Falotico R, Jaeger J, Popma JJ, Serruys PW. Lack of neointimal proliferation after implantation of sirolimus-coated stents in human coronary arteries: a quantitative coronary angiography and three-dimensional intravascular ultrasound study. Circulation 2001;103:192–5.

[25] Kastrati A, Schomig A, Dirschinger J, Mehilli J, von Welser N, Pache J, Schuhlen H, Schilling T, Schmitt C, Neumann FJ. Increased risk of restenosis after placement of gold-coated stents: results of a randomized trial comparing gold-coated with uncoated steel stents in patients with coronary artery disease. Circulation 2000;30:2478–83.

[26] Edelman ER, Seifert P, Groothuis A, Morss A, Bornstein D, Rogers C. Gold-coated NIR stents in porcine coronary arteries. Circulation 2001;103:429–34.

[27] Nakayama Y, Ji-Youn K, Nishi S, Ueno H, Matsuda T. Development of high performance stent: gelatinous photogel-coated stent that permits drug delivery and gene transfer. J Biomed Mater Res 2001;57:559–66.

[28] Holmes DR, Camrud AR, Jorgenson MA, Edwards WD, Schwartz RS. Polymeric stenting in the porcine coronary artery model: differential outcome of exogenous fibrin sleeves versus polyurethane-coated stents. J Am Cardiol 1994;24:525–31.

[29] Severini A, Mantero S, Tanzi MC, Cigada A, Salvetti M, Cozzi G, Motta A. Polyurethane-coated, self-expandable biliary stent; an experimental study. Acad Radiol 1995;2:1078–81.
[30] Castaneda F, Ball SM, Wyffles PL, Young K, Li R. Assessment of a polyester-covered nitinol stent in an atherosclerotic swine model. J Vasc Interv Radiol 2000;11:438–91.
[31] Schellhammer F, Berlis A, Bloss H, Pagenstecher A, Schumacher M. Poly-lactic acid coating for endovascular stents. Preliminary results in canine experimental arteriovenous fistulae. Invest Radiol 1997;32: 180–6.
[32] Hietala EM, Salminen US, Stahls A, Valimaa T, Maasilta P, Tormala P, Nieminen MS, Harjula AL. Biodegradation of the copolymeric polylactide stent. Long-term follow-up in a rabbit aorta model. J Vasc Res 2001;38:361–9.
[33] Tamai H, Igaki K, Kyo E, Kosuga K, Kawashima A, Matsui S, Komori H, Tsuji T, Motohara S, Uehata H. Initial and 6-month results of biodegradable poly-L-lactic acid coronary stents in humans. Circulation 2000;102:399–404.
[34] Petas A, Vuopio-Varkila J, Siitonen A, Valimaa T, Talja M, Taari K. Bacterial adherence to self-reinforced polyglycolic acid and self-reinforced polylactic acid 96 urological spiral stents in vitro. Biomaterials 1998;19:677–81.
[35] Ozbek C, Heisel A, Gross B, Bay W, Schieffer H. Coronary implantation of silicone-carbide-coated Palmaz–Schatz stents in patients with high risk of stent thrombosis without oral anticoagulation. Catheter Cardiovasc Diagn 1997;41:71–8.
[36] Beythien C, Gutensohn K, Bau J, Hamm CW, Kuhnl P, Meinertz T, Terres W. Influence of stent length and heparin coating on platelet activation: a flow cytometric analysis in a pulsed floating model. Thromb Res 1999;94:79–86.
[37] Etave F, Finet G, Boivin M, Boyer JC, Rioufol G, Thollet G. Mechanical properties of coronary stents determined by using finite element analysis. J Biomech 2001;34:1065–75.
[38] Hendey B, Klee CB, Maxfield FR. Inhibition of neutrophil chemokinesis on vitronectin by inhibitors of calcineurin. Science 1992;258: 296–9.
[39] Hendey B, Maxfield FR. Regulation of neutrophil motility and adhesion by intracellular calcium transients. Blood Cells 1993;19:143–64.

ELSEVIER

Cardiovascular Radiation Medicine 4 (2003) 29–33

CARDIOVASCULAR RADIATION MEDICINE

Embolization of experimental aneurysms using a heparin-loaded stent graft with micropores

Shogo Nishi[a,*], Yasuhide Nakayama[b], Hatsue Ueda-Ishibashi[c], Takehisa Matsuda[d]

[a] *Department of Neurosurgery, Takatsuki Red Cross Hospital, 1-1-1 Abuno, Takatsuki, Osaka 569-1096, Japan*
[b] *Department of Bioengineering, National Cardiovascular Center Research Institute, 5-7-1 Fujishiro-dai, Suita, Osaka 565-8565, Japan*
[c] *Department of Pathology, National Cardiovascular Center Hospital, 5-7-1 Fujishiro-dai, Suita, Osaka 565-8565, Japan*
[d] *Department of Biomedical Engineering, Graduate School of Medicine, Kyushu University, 3-1-1 Maidashi, Higashi-ku, Fukuoka 812-8582, Japan*

Received 24 March 2003; accepted 24 March 2003

Abstract

Purpose: For percutaneous transluminal angioplasty (PTA), a heparin-loaded stent graft, composed of a commercially available metallic stent with a microporous and surface-modified thin film, has been developed. Early controlled endothelialization is promoted by a regular array of micropores produced by an excimer laser ablation technique. Early thrombus is prevented by a drug delivery system established by impregnation of photoreactive gelatin with heparin. Our stent grafts were used for embolization of experimental carotid aneurysms with an autologous external jugular vein patch in dogs.
Materials and methods: At 1 month after formation, the aneurysms were occluded with stent grafts. Affected arteries were removed with the aneurysms, immediately (two aneurysms in one dog), 1 week (four aneurysms in two dogs), 1 month (three aneurysms in two dogs) and 3 months (four aneurysms in two dogs) after embolization, and were studied histologically to evaluate patency and endothelialization over the intraluminal surface of the thin film.
Results: Treated carotid arteries were all patent with occluded aneurysms completely at any periods. Even at 1 week after embolization, endothelialization was confirmed on the surface of the stent graft on the lumen side. At 1 and 3 months, all treated aneurysms with enough patent parent arteries were filled with organized tissues and completely occluded.
Conclusion: Our developed stent graft appears to be promising for the treatment of aneurysms, especially with respect to immediate termination of blood inflow and early endothelialization in the neck of the aneurysm.

Keywords: Stent graft; Micropores; Heparin; Experimental aneurysm; Carotid artery

1. Introduction

Improvement in endovascular techniques for the treatment of intracranial aneurysms with GDC coils has led to excellent clinical results [1–3]. However, intrinsic technical problems remain, especially for the occlusion of surgically difficult large or giant aneurysms [4]. Complete occlusion of broad-based aneurysms may be hazardous because misplaced occlusive material may enter and block the parent vessel. Thromboembolic complications also occur, and neck remnants may cause regrowth of the aneurysm and rupture.

Our stent graft consists of a metallic stent, a microporous cover and a local drug delivery system for heparin. Early induction of intraluminal endothelialization and control of tissue ingrowth from surrounding tissues are assured by the micropores. In this study, our stent grafts were used for embolization of experimental carotid aneurysms in dogs. We showed satisfactory occlusion of

* Corresponding author. Tel.: +81-72-696-0571; fax: +81-72-696-1228.
E-mail address: snishi@ja3.so-net.ne.jp (S. Nishi).

1522-1865/03/$ – see front matter © 2003 Elsevier Inc. All rights reserved.
doi:10.1016/S1522-1865(03)00114-8

the aneurysms, together with prevention of early occlusion and late patency of the parent artery.

2. Materials and methods

Thirteen experimental saccular aneurysms [5] were created in seven adult mongrel dogs, each weighing about 13–15 kg. The aneurysms measured 0.5 cm in diameter at the neck and 1.0 cm in height. The high-performance stent grafts were metallic stents (Palmaz stent; Cordis, Johnson & Johnson, Japan) bearing a thin microporous segmented polyurethane (SPU) film impregnated with heparin [6]. They were placed in the common carotid artery across the aneurysms on both sides. Aspirin and ticlopidine were administered orally at a dosage of 81 and 100 mg once daily, respectively, from 1 week prior to creation of the aneurysms. Angiography was performed before stent graft placement, immediately after deployment of stent grafts, and 1, 4 and 12 weeks after stenting.

2.1. Fabrication of the stent graft

Micropores were formed on a SPU thin film by using an excimer laser ablation technique [7]. The pore size was 100 μm, and the interpore distance was 250 μm. After formation of micropores, 1 mg (164.5 units)/cm^2/10 μl heparin was impregnated onto the surface of the film by photoreactive gelatination. With the aid of a microscope, the modified film was sutured on the stent strut with 10.0 nylon thread, rolled up and fixed on it with *N,N*-dimethylformamide solvent (Fig. 1).

2.2. Preparation of aneurysms in dogs

Lateral-wall vein-patch aneurysms with a 5-mm orifice were constructed bilaterally in the common carotid arteries of seven adult mongrel dogs [5,8]. A total of 13 aneurysms were created. Surgical procedures were performed under a protocol approved by our institution's Animal Care Committee. The dogs were maintained on standard laboratory diet. The dogs were anesthetized with intramuscular injection of Ketalar (1 cc/kg) and atropine sulfate (0.5 mg), endotracheally intubated and maintained with 20–30 mg/kg sodium pentobarbital iv. A 10-cm cervical midline skin incision, dissection of the muscles and connective tissues exposed the bilateral common carotid arteries and the right external jugular vein. Two pieces of the external jugular vein were harvested. The carotid arteries were cleared of adventitia and were clamped on both sides. A longitudinal linear arteriotomy was made. The vein graft was then sutured onto the artery with a discontinuous 8.0 nylon suture (Fig. 2). Seven dogs each had one aneurysm on each carotid artery.

2.3. Procedure for embolization of aneurysm

The balloon expandable stent with microporous SPU film impregnated with heparin was mounted on the percutaneous transluminal angioplasty (PTA) balloon (a 5 French Power Flex PTA balloon 4 or 5 mm, 2 cm; Cordis, Johnson & Johnson) after sterilization using 0.5% Maskin-alcohol before use. Aneurysms were embolized using our stent graft, 2–4 weeks after creation. The femoral artery was surgically exposed. A 6 French sheath introducer was

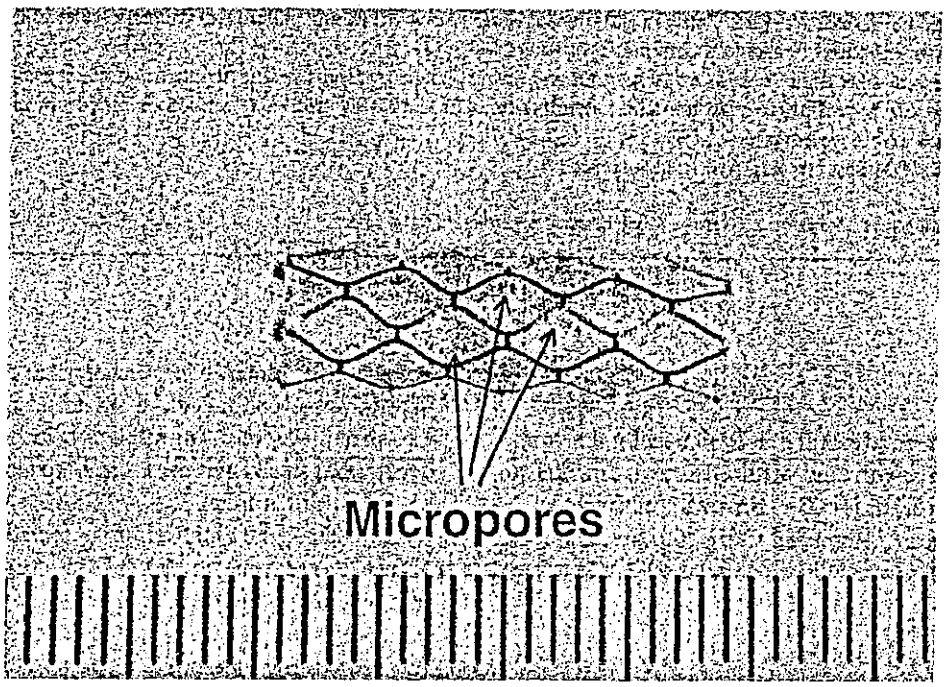

Fig. 1. An expanded stent graft. Ovoid-shape micropores are seen on the inflated and detached stent graft.